EFFECTS OF INTERNAL AND EXTERNAL FACTORS ON INTERSPECIFIC COMPETITIVE ABILITIES OF PHYTOPLANKTON ASSEMBLAGES INFLUENCED BY ALLELOPATHY

A Dissertation

by

RIKA MARIE WANDLESS MUHL

Submitted to the Office of Graduate and Professional Studies of
Texas A&M University
in partial fulfillment of the requirements for the degree of

DOCTOR OF PHILOSOPHY

Chair of Committee,	Daniel L. Roelke
Committee Members,	Rusty Feagin
	Anna Armitage
	Dan C.O. Thornton
Head of Department,	David Caldwell

May 2018

Major Subject: Wildlife and Fisheries Sciences

ABSTRACT

Phytoplankton allelopathic processes operate on short time scales, and some allelopathic species can alter phytoplankton succession and affect biodiversity. Both internal and external factors have a role in these processes.

Succession under allelopathic influence often results in dominance of the allelopathic species, and this research shows that how quickly an assemblage transitions from the effects of interference competition to exploitative competition is influenced by the similarity of life history traits of phytoplankton in an assemblage.

Ecologists accept that competition is invoked as resources become limiting; however, when co-occurring species are competitively similar, competition effects may be reduced. Using a mathematical model of phytoplankton competing for limiting resources for three types of assemblages, I found that intransitive assemblages yield the highest relative biodiversity, followed by lumpy assemblages, and neutral assemblages the lowest biodiversity. Testing these modelling results with empirical data from eight freshwater systems supports the idea that assemblages characterized by lumpiness are more resistant to blooms of allelopathic species than assemblages that are not as lumpy.

Field experiments manipulating toxicity of the allelopathic phytoplankter *Prymnesium parvum* using different pH levels demonstrate the significance of biologic controls on the bloom potential of allelopathic species. Treatments with large zooplankton suppressed the population density of this haptophyte in waters from Galveston and Matagorda Bays.

These results may aid our understanding of broad themes in harmful algae ecology, including how ecosystems respond to disturbances such as allelopathy.

DEDICATION

This is dedicated to those who strive to give more than they take and who desire to put their knowledge into action.

ACKNOWLEDGEMENTS

I am grateful to many people and institutions that have provided encouragement and assistance to me in this research. My committee members Dan Roelke (chair), Rusty Feagin, Anna Armitage and Dan Thornton for their comments that truly made this dissertation a better and more thoughtful effort. I am especially grateful to my committee chair, Dan, who invited me into his lab and showed me the wonders held in a single drop of water.

Sparky Umprhres, Veronica Lundgren and Sierra Cagle deserve a special mention for help sampling and lugging heavy carboys around on long trips to the Texas coast. I am thankful to Texas Parks and Wildlife for letting me use their facilities at Port O'Connor as a "visiting researcher" and for the resident osprey there, adding an unexpected element of joy in the field. I am thankful to the Bryan Brooks lab at Baylor University for processing samples for toxicity analysis, and to Casan Scott for meeting me at odd hours with that handy cart. A special thank you to the Antoinetta Quigg lab at TAMU-Galveston for use of her lab during the Galveston experiments.

I am forever thankful to my parents, J.I. and Shelby, and my brother, Berry, and my sister, Juli, who have been excited and interested in what I did this go around.

CONTRIBUTORS AND FUNDING SOURCES

Contributors

This work was supported by a dissertation committee consisting of Professor Daniel Roelke of the Department of Wildlife and Fisheries Sciences, Professors Rusty Feagin and Anna Armitage of the Department of Ecosystem Sciences and Management, and Professor Dan Thornton of the Department of Oceanography.

The mathematical algorithm used in Chapter 3 was written in part by Joydeb Bhattacharya of the Department of Mathematics, Karimpur Pannadevi College, India. The time series data in Chapter 4 was contributed by Tamar Zohary of the Israel Oceanographic and Limnological Research Institute, Gábor Borics of the Danube Research Institute, Maria Moustaka-Gouni of the Aristotle University of Thessaloniki, Ursula Gaedke of the University of Potsdam and Ulrich Sommer of the Helmholtz Centre for Ocean Research.

All other work conducted for the dissertation was completed by the student independently.

Funding Sources

Graduate study was supported by a fellowship of the National Fish and Wildlife Foundation Conservation Scholars Program and a grant from Texas Sea Grant, Grants-In-Aid of Graduate Research Program.

TABLE OF CONTENTS

LIST OF FIGURES

Page

LIST OF TABLES

Page

CHAPTER I

INTRODUCTION

Competition for resources--light, space, nutrients--drives phytoplankton interactions, and phytoplankton can employ mechanisms for maximizing access to resources in the presence of competitors. Allelopathy is a form of interference competition, and is thought by phytoplankton ecologists to be more evident among species that are poor competitors for limiting resources (Legrand et al., 2003.) Allelopathic effects are not the same for all phytoplankton and some taxa may be more sensitive to toxins than others (Fistarol, 2003; Hattenrath-Lehman and Gobler, 2011). Allelopathic interaction can create turnover in species dominance, with the allelopathic species often capable of creating monospecific blooms. These blooms often become harmful, either through direct toxicity that kills or exerts sublethal effects on other species; or by shading other autotrophs in the water column and preventing their access to light; or by reducing the available oxygen in the system as a result of decomposition processes. These are well-known effects, yet allelopathic effects in aquatic systems are far from straightforward and predictable.

Researchers have found that allelopathy can prevent competitive exclusion and maintain biodiversity in phytoplankton assemblages through population dynamics in which no single species can outcompete all others (Felpeto et al., 2018). This supports many field observations of highly diverse phytoplankton assemblages during allelopathic blooms. I discuss how population dynamics among phytoplankton can influence allelopathic interactions and competitive outcomes in Chapters 2 and 3. Distinguishing between the effects of exploitative and interference competition for resources becomes crucial in order to appreciate the underlying mechanism of allelopathic influence presented in this research. The research presented in these chapters moves beyond the solid conceptual thinking of competition between a few species in spatial or temporal

isolation, and looks at the relationship between all assemblage members as a relevant factor in competitive outcome. In Chapter 4, I describe my experiments with the allelopathic invasive phytoplankton species *Prymnesium parvum* in two Texas estuaries, and discuss its potential to broaden its range in Texas.

Considering that there are many strategies phytoplankton use to secure resources for their growth and survival, we may ask "just what is allelopathy"? A broad definition includes both inhibitory and stimulatory effects by one species on another (Rice, 1984), and applied to terrestrial systems, the term can have positive connotations, in part because it is commonly used as a strategy to increase crop yield (Rice 1984; Jimenez-Osornio 1987). Aquatic ecologists describe allelopathy as the negative effect of a species on another, with recent efforts to further narrow its meaning to exclude zooplankton and pathogens (Legrand et al., 2003). At times, it is difficult to escape confusion on the issue, especially as published research and observations over the last several decades discuss "anti-microbial", "anti-biotic", "nuisance", "noxious", "harmful", "chemically-mediated" and "toxic" effects of chemical compounds. Sometimes this discussion occurs in reference to interspecies competition, and may then describe chemical compounds as "exogenous", "extracellular, "exuded", "endogenous", "intracellular" or "secondary metabolites" to describe the source of a toxin, and by implication whether interference competition is being invoked. As methodologies have improved and interpretations are refined, our phrasing of these phenomena has changed and become more contextualized. In this dissertation, I use the word allelopathy to refer to the effect of exuded chemicals of phytoplankton species on other phytoplankton species, though I find it relevant at times to use "toxic" or "harmful algal bloom" (HAB).

References

Felpeto, A., Roy, S. Vasconcelos. 2018. Allelopathy prevents competitive exclusion and promotes phytoplankton biodiversity. Oikos, 127:1, 85-98.

Fistarol, G.O., Legrand, C., and Grane´li, E., 2003. Allelopathic effect of Prymnesium parvum on a natural plankton community. Marine Ecology Progress Series 255, 115–125.

Hattenrath-Lehmann, T.K., C.J. Gobler. 2011. Allelopathic inhibition of competing phytoplankton by North American strains of the toxic dinoflagellate, *Alexandrium fundyense*: Evidence from field experiments, laboratory experiments, and bloom events Harmful Algae 11, 106–116

Jimenez-Osornio, J.J. and S.R. Gliessman. 1987. In Allelochemicals, Role in Agriculture and Forestry (G.R.Waller, Ed.), Vol. 300, American Chemical Society, Washington, DC, pp 262-274.

Legrand C, Rengefors K, Fistarol GO, Granéli E (2003) Allelopathy in phytoplankton—biochemical, ecological, and evolutionary aspects. Phycologia 42:406–419

Rice, E.L. 1984. *Allelopathy*, ed. 2, Academic Press, New York, 424 pages.

CHAPTER II

MODELING RELATIONSHIPS BETWEEN PHYTOPLANKTON ALLELOPATHY, FUNCTIONAL TRAIT DISSIMILARITY AND SELF-ORGANIZED BIODIVERSITY

An underlying assumption of competition theory is that when resources become limiting, competition for those resources is invoked, benefiting species that have lower requirements for the limiting resource (Tilman 1977, 1982; Keddy 1989). Species that are poor exploiters of resources such as nutrients may employ physical or chemical interference strategies to gain access to resources (Case and Gilpin 1974). With phytoplankton, an active behavior to enhance nutrient acquisition employed by some species is allelopathy (Smayda 1997; Thornton 2014; Legrand et al. 2003).

Allelopathy in aquatic ecology is defined as the negative effect of exuded chemicals on the growth and fitness of species of the same trophic level (Legrand et al. 2003; Hattenrath-Lehmann et al. 2011). Negative effects could involve lysis of competitors, after which the allelopathic species might capture cell fragments through phagotrophy or uptake liberated cellular compounds through osmotrophy (Uronen et al. 2007). This negative effect could also involve reducing photosynthetic efficiency of competitors, thus reducing growth (Sukenik et al., 2002; Prince et al. 2008). Alternatively, the allelopathic species might simply benefit from stimulated microbial regeneration of nutrients from lysed cells that then become available for reuse (Uronen et al. 2007).

While the *prima facie* cornerstone of allelopathic ecological understanding is that allelopathy facilitates bloom formation by reducing competitor density and subsequently increasing nutrient availability for the allelopathic species (Smayda 1997; Lewis 1986; Jonsson et al. 2009; Legrand et al. 2003; Fistarol et al. 2003), experimental and field observations of

allelopathy within phytoplankton assemblages reveal a wide spectrum of effects and varying sensitivities among taxa to allelochemicals (Hattenrath-Lehmann et al. 2011). These include positive associations. For example, pairwise interactions with the allelopathic dinoflagellate *Karenia brevis* have shown differential effects within an assemblage where some members are negatively affected and others positively (Poulson et al. 2010). Similarly, stimulatory effects to other phytoplankton have been observed with allelopathic cyanobacteria and dinoflagellates (Suikkanen et al. 2005; Poulson et al. 2010; Neisch et al. 2012). Succession during some allelopathic blooms is complex, with observed co-dominance of species (Redlaje 2003; Lindholm et al. 1999) and persistence of multiple sub-dominant species (West et al. 1996; Figueiredo et al. 2006) during allelopathic blooms. This known variation of allelopathic effects spotlights our limited understanding of allelopathic functioning in ecosystems.

Some of the road blocks to further understanding allelopathic functioning in plankton systems may also arise from our limited knowledge of phytoplankton assemblage structure, and how this structure relates to the degree of exploitative competition occurring within assemblages, which I now refer to as the 'competitive power' of the assemblage. Here, 'structure' refers to the competitive abilities of assemblage members to exploit resources relative to each other, which is typically depicted by the distribution of R* values through the resource trade-off space (discussed further below). In theory, this type of structure characterization is related to biodiversity, succession dynamics, productivity and stability of the assemblage (Tilman 1994; Chase and Leibold 2014). Assuming that assemblage structure influences the efficacy of allelopathy, yet is not considered when analyzing field observations, then allelopathic effects could be masked by noise in observational data. So then, does assemblage structure influence allelopathy efficacy? Here, I explore that question with a focus on assemblages whose structure

derives from generalized ecological concepts relating to competition, which are neutrality, lumpy coexistence and intransitivity.

The neutral theory of biodiversity describes interactions of species of the same trophic level in which the similarity of life history traits nullifies competitive phenomena, allowing coexistence (Hubbell 2005). In this view, diversity can be explained when the fitness of all individuals in an assemblage is the same and spatial heterogeneity is explained by stochastic events. For example, the random allocation of space for dispersing larvae of coral reef fish promotes species coexistence through variability in birth rate, irrespective of competitive abilities of species (Sale 1977; Chesson and Warner 1981). Neutrality has also been suggested as a mechanism underlying high species richness in phytoplankton assemblages (Roelke and Eldridge 2008; Chust et al., 2013).

Lumpy coexistence describes a condition where traditional niche-based competition and neutral theory are reconciled. In this condition, species self-organize into multiple clusters along resource gradients, in which members of a cluster are competitively neutral and clusters compete for resources (Holling 1992; Scheffer & van Nes 2006; Fort & Scheffer 2010). Evidence of lumpy coexistence in natural systems includes observations of species arranging themselves along a body size gradient (an analog to resource gradient) into discrete clusters (see Scheffer & Van Nes 2006). Size distributions in nature are associated with life history traits, although relationships can be complex (Marquet 2000; Litchman et al. 2007; Sommer et al. 2017). For example, large-scale seasonal sampling of freshwater plankton in lakes in Wisconsin shows similarity in the organization of lumps and gaps across similar size ranges despite lake system differences (Havlicek et al. 2001). This phenomenon has been observed in other assemblages of

phytoplankton, zooplankton and aquatic beetles, and in terrestrial systems with prairie birds and forest mammals (Drost et al. 1992; Holling 1992; Segura et al. 2011, 2013).

A third generalized ecological concept describes a condition involving intransitivity. In plankton systems, this can come about when multiple species co-occur in which each is a superior competitor for a different resource, but each species also has a high demand for a resource for which a co-occurring species is the superior competitor. This leads to a condition in which a dominant species undermines its own persistence. Stated more specifically, imagine a system with three species and three resources, where species A, B and C are superior competitors for resources 1, 2 and 3, respectively, and these species have the highest demand for resources 2, 3 and 1, respectively. An initial condition of resource 1 limitation in such a system would lead to the dominance of species A. But protracted dominance of species A would bring about limitation of resource 2, thereby giving species B a competitive advantage, eventually leading to its dominance. Protracted dominance of species B would bring about limitation of resource 3, leading to eventual dominance of species C, which would eventually bring about limitation of resource 1. Thus, the cycle repeats (A-B-C-A-B-C-etc.), sustaining biodiversity over time (Gilpin 1975; Frean & Abraham 2001). Intransitive dynamics can occur when competition is non-hierarchical like this. Intransitive dynamics have been demonstrated by several modeling studies (Karlson & Jackson 1981; Durret and Levin 1997; Nakamaru & Iwasa 2000; Czaran et al. 2002; Laird & Schamp 2006). In addition, multiple species that are similarly able to compete for a resource may coexist with these intransitive dynamics. For example, a recurrent succession pattern could be A-BD-CE-A-etc. where species B and D, and species C and E are competitively similar (Huisman and Weissing 2001; Roelke et al. 2003). Analogous evidence of intransitive dynamics from natural systems includes observations of sessile communities on coral reefs (Buss

and Jackson 1979), herbaceous dicots examined along a resource gradient (Fortner and Weltzin, 2007) and reproductive strategies of male side-blotched lizards (Sinervo and Lively, 1996). Intransitivity has also been suggested as a mechanism underlying high species richness in phytoplankton assemblages (Huisman & Weissing 1999; Schippers 2001; Roelke & Eldridge 2008). Experimentally, intransitivity was demonstrated in a microbial system, where a highly toxic strain of *Escherichia coli* was displaced by a toxin-resistant, non-toxic, slow-growing strain; which was then displaced by a toxin-sensitive, non-toxic, fast-growing strain; only to be displaced by the original toxic strain (Kerr et al., 2002).

Effects of allelopathy on phytoplankton are diverse, and our limited understanding of underpinning mechanisms might be, in part, a function of our lack of knowledge of distinctive assemblage structures occurring in natural environments. Researchers acknowledge that methodologies for study of sensitivities of individual phytoplankton species to allelopathic compounds overlook assemblage dynamics (Kubanek et al. 2005), and experiments exploring allelopathic influence on natural assemblages do not directly relate allelopathy and assemblage state (Poulson et al. 2010; Tang and Gobler 2010; Poulson et al. 2014). I address that here by employing mathematical models to explore the interaction of allelochemical production rate and target species sensitivity on diversity in assemblages governed by neutrality, lumpy coexistence and intransitivity. Emergent behavior of the combined models is then tested using phytoplankton time-series data from several lakes of varied morphometry and trophic state.

Methods

For my modeling, I started with a well-known numerical model that depicts multiple phytoplankton species competing for multiple growth-limiting resources (Leon and Tumpson 1975; Tilman et al. 1982; Grover 1997). The model is dimensionless (box model), employing

time-dependent ordinary differential equations. To the phytoplankton equations of this model, I added a factor depicting an allelopathic effect (deleterious) on the growth of non-allelochemical

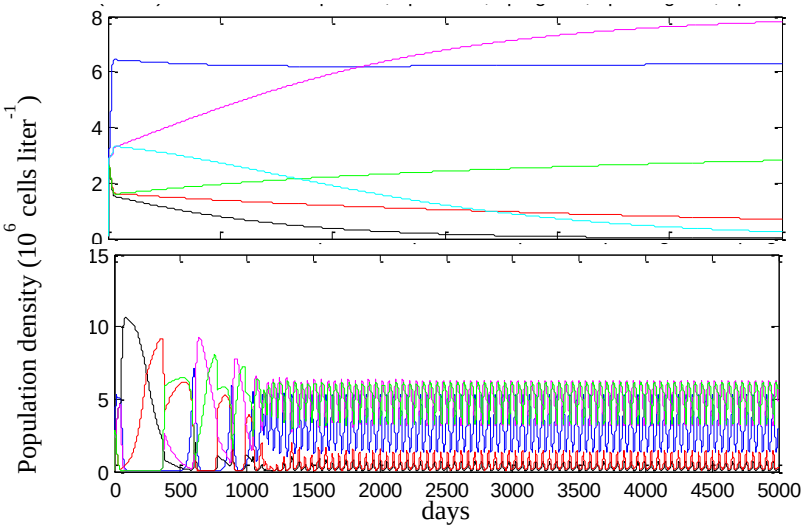

Figure 2.1. Representative simulations for neutral and lumpy assemblages (a), and for intransitive assemblages (b), showing the model asymptotically approaching a steady state when assemblages are neutral or lumpy, and showing a period of transient dynamics giving way to an oscillating state when assemblages are intransitive. In these simulations there are no allelopathic effects.

producers. In addition, I added a differential equation that depicted the concentration of the allelochemicals where increases in concentrations occurred through production by the allelochemical species and decreases in concentration were through a fixed rate of decay (Martines et al. 2009). Thus, I considered only the effect of one allelopathic species on multiple non-allelopathic species, although I acknowledge that phytoplankton assemblages will likely have more than one allelopathic species, that allelopathic species can affect each other, and that there are likely competitive tradeoffs associated with being allelopathic, all of which could be explored in future research, but are beyond the scope of the current study.With this expanded

model, I explored how the structure of phytoplankton assemblages influenced allelopathy efficacy. For this purpose, I used biodiversity collapse (richness reducing to one, where the sole surviving species was the allelopathic species) to define under which scenarios allelopathy led to blooms. The scenarios explored here were based on the sensitivity of assemblage members to allelochemicals and the rate of allelochemical production. Assemblages used in these analyses (reported in Roelke and Eldridge 2008), in the absence of allelopathy, were species supersaturated, meaning the number of co-existing species at steady-state exceeded the number of limiting resources (Schippers et al. 2001). Species supersaturation (ranging between 5-8 species co-existing on three resources) was sustained by either neutrality, lumpy coexistence, or intransitivity.

Regarding resources, parameterizations in the model concerning the first resource are based on nitrogen, which included loading, half-saturation coefficient for phytoplankton growth and cellular composition (discussed further below). Parameterizations concerning the other resources were assigned comparable values, and so should be viewed as other growth limiting resources expressed in units of nitrogen-equivalents. A detailed description of the self-organization process used to generate supersaturated assemblages can be found in Roelke & Eldridge (2008). Population dynamics for these assemblage types in the absence of allelopathy either asymptotically approached a steady state when sustained by either neutrality or lumpy coexistence (Figure 1 top panel), or showed recurrent and out-of-phase species oscillations when sustained by intransitivity (Figure 1 bottom panel).

Mathematical Model and Numerical Solution

Demographics of phytoplankton species were modeled using two equation forms, one form (eq. 1) for the allelochemical producer and the other form (eq. 2) for non-allelochemical producers, which were:

$$\frac{dN_1}{dt} = \mu_1 N_1 - vN_1 \quad (1)$$

$$\frac{dN_{2-s}}{dt} = \mu_{2-s} N_{2-s} (\frac{KI}{C + KI}) - vN_{2-s} \quad (2)$$

in which N_1 was the population density of the allelopathic species ($x10^6$ cells L^{-1}), $N_{2\text{-}s}$ were the respective population densities of the target species in which *s* was the total number of species in the assemblage, μ was the specific growth rate (day^{-1}), and *v* was the continuous flushing rate (day^{-1}). Parameters KI ($\mu g\ L^{-1}$) and C ($\mu g\ L^{-1}$) depicted allelopathic effects, where KI was the growth inhibition of the non-allelopathic species by allelochemicals (larger values equating to less sensitivity to toxins) and C was the concentration of the allelochemical.

Changes in allelochemical concentration were represented by the equation:

$$\frac{dC}{dt} = \mu N_1 \varepsilon_c - k_c C \quad (3)$$

where ε_c was the allelochemical production coefficient ($\mu g\ cell^{-1}$) and k_c was the allelochemical decay coefficient (day^{-1}).

As with previous iterations of the model, μ of each phytoplankton species was determined using the Monod equation and Liebig's law of the minimum, with equations of the form:

$$\mu = \mu_{\max} (\min[\frac{R_1}{R_1 + k_{R_1}}, \frac{R_2}{R_2 + k_{R_2}}, \frac{R_3}{R_3 + k_{R_3}}]) \quad (4)$$

in which μ_{max} was the maximum specific growth rate (day $^{-1}$) of each species, R_1, R_2, and R_3 were the concentrations of resources 1, 2 and 3 (μmol L^{-1}), and $k_{R_{1-3}}$ were the half-saturation coefficients for resource-limited growth (μmol L^{-1}). A function 'min' was used to determine which resource was most limiting to growth during simulations.

Changes in resource concentrations used equations of the form:

$$\frac{dR}{dt} = v(R_{in} - R) - \sum_{i=1}^{s} Q_i \mu_i N_i \quad (5)$$

in which Q_i was the fixed cellular content of the resource (μmol cell^{-1}) for any species *i*, R_{in} was the fixed concentration of the resource in the supply (μmol L^{-1}), and other parameters are the same as previously described. Differential equations were solved numerically using ordinary differential equation solving routines part of a commercial software package (MATLAB from The Mathworks, Inc.). The routines are based on 4th order Runge-Kutta methods, and used a variable time step that was based on a local error tolerance set at 10^{-6}.

Model Parameterization

For all simulations, phytoplankton life-history traits were parameterized based on previous research (Roelke & Eldridge 2008), which followed self-organization from species rich pools guided by various ecological principals. Thirty assemblages that were previously shown to be supersaturated, whereby the number of coexisting species is greater than the number of limiting nutrients, were used in simulations (Schippers et al. 2001; see Appendix of Roelke & Eldridge 2008). Of these, ten assemblages were comprised of species that were competitively neutral, ten assemblages were characterized by lumpy coexistence, and ten assemblages were characterized by intransitive population dynamics. The half-saturation constants (k_R) and fixed

cellular contents (Q) were different for each species in each assemblage. Values for k_R and Q for all of the assemblages can be found in the Appendix of Roelke & Eldridge (2008).

Conceptual Framework

Competitive abilities of species in each assemblage type are demonstrated with a three-dimensional resource trade-off space using the R* for each species for each of the three resources (Roelke and Eldridge 2008). R* was determined using the equation:

$$R^* = \frac{vk_R}{\mu_{\max} - v} \tag{6}$$

in which the parameters are the same as previously described. The distribution of species' R*s through the three-dimensional resource trade-off space is used to define the assemblage structure. For example, all species in neutral assemblages show close clustering in the resource trade-off space (Figure 2a). Species in assemblages characteristic of lumpy coexistence also show close clustering of species, but with co-occurrence of multiple species clusters within the three-dimensional trade-off space (Figure 2b). Species in intransitive assemblages were characteristic of a recognizable geometric species distribution with assemblage members being near-equal distant to a species located in the "central" region of the three-dimensional trade-off space (Figure 2c, d).

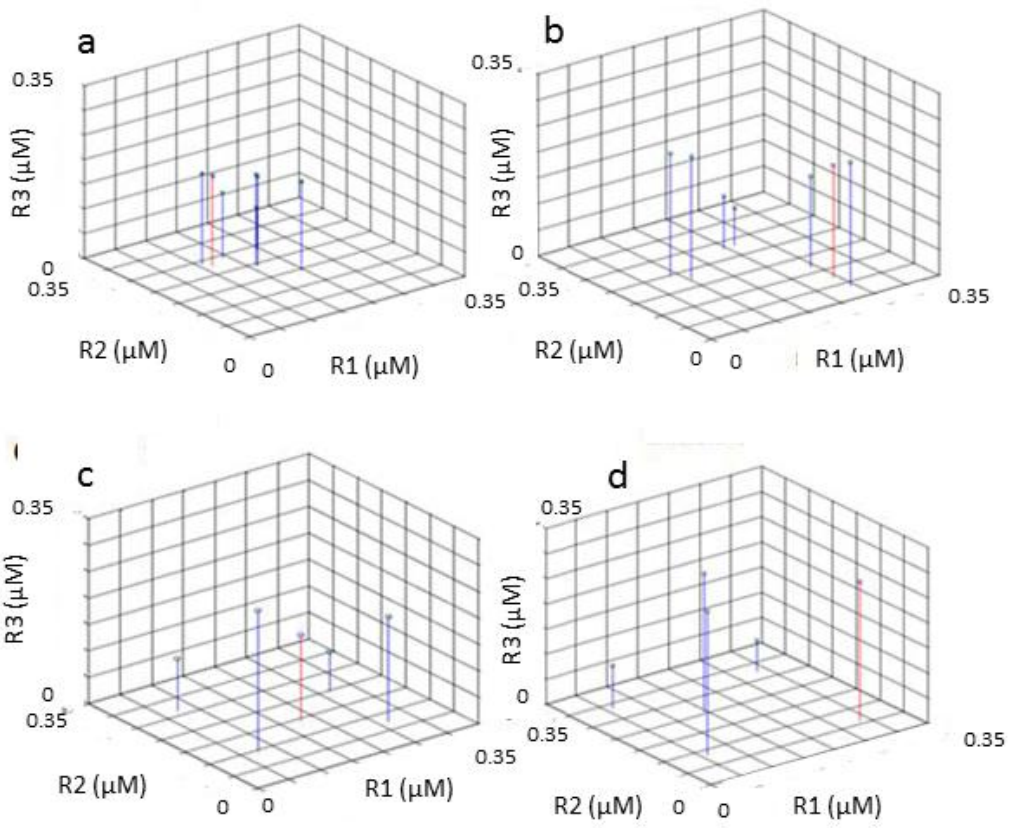

Figure 2.2. Representative distributions of species' R*s through the three-dimensional resource trade-off space for neutral (a), lumpy (b) and intransitive (c, d) assemblages. The three resources are designated with R1, R2 and R3. Here, the position of the R*s for the allelopathic species is denoted with a grey dashed line and dot, while non allelopathic species are denoted with a black line and dot. Note that in some simulations employing intransitive assemblages the allelopathic species was centrally located among the other species of the assemblage (c) and for other simulations it was peripherally located (d).

Sensitivity Analysis of Model

I explored the resistance of phytoplankton assemblages to allelopathy by looking at how an allelopathic species influences assemblage diversity over a gradient of allelopathic effect. I varied ε_c, the allelochemical production value, and KI, the growth-inhibition coefficient, for which low values of KI represented extreme growth-inhibition of the non-allelopathic species, and high values of KI represented less inhibition. This resulted in varying levels of sensitivity to the allelochemical by the non-allelochemical producers. A gradient of 12 values used for ε_c

ranged from 0 to 0.055, which spanned allelochemical production rates observed previously for cyanobacteria (Grover et al. 2010). A gradient of 100 values was used for KI, ranging from 0 to 1. During preliminary simulations I observed that values > 1 for the growth inhibition coefficient showed no effect of allelopathy. So those simulations are not reported here.

Each simulation started with the full number of species in the assemblage and ran for 5000 days. For neutral and lumpy assemblages, starting species richness was between six and eight species, whereas for the intransitive assemblages, five species were used. Because the number of species in these assemblage types varied initially, I analyzed relative diversity instead of diversity (see more below). Using the relative diversity calculations, biodiversity maps were created. These maps displayed the resulting relative diversity of each assemblage at all possible combinations of ε_c and KI (1212 model simulations for each map). The biodiversity maps show changes in relative diversity in response to allelopathy. For example, when viewing a map from right to left, transition from a stable multispecies assemblage when KI values were large to an allelopathic monoculture when KI values were small is seen. When viewing a map from bottom to top, transition from a stable multispecies assemblage when ε_c values were low to an allelopathic monoculture when ε_c values were large is seen. A transition slope, which combined trends from KI and ε_c, was then calculated where assemblages' resistance to allelopathy were determined, with low slopes indicating less resistance and steeper slopes indicating greater resistance.

Initial Condition of Models

Following Roelke and Eldridge (2008), initial phytoplankton densities (N) were 0.1 (x 10^6 cells L^{-1}) for all species in all model runs, maximum growth rates (μmax) were 1 day^{-1}, initial concentrations for all resources (R) were 10 μmol L^{-1} and flushing rate (v) was 0.25 day^{-1}.

For neutral and lumpy assemblages, the species from the existing assemblage selected to be allelopathic was arbitrary. For intransitive assemblages, the species from the existing assemblage selected to be allelopathic was first centrally located among the five species in the resource trade-off space (Figure 2c), and then simulations run again where the allelopathic species was peripherally located (Figure 2d).

Assemblage Characteristics of Interest and Emergent Behavior

Relative species diversity, relative assemblage cell density, assemblage resistance and the averaged distance of each species from the allelopathic species in the resource trade-off space were determined for the thirty assemblages. These factors provide a context for ecological study at different levels of interspecific competition, although assemblage response to allelopathy will involve multiple factors in natural systems.

Diversity values were calculated using the Shannon-Weiner diversity index (Shannon and Weaver 1948) and modeled using the equation:

$$H' = -\sum_{i=1}^{s} p_i \log_2(p_i) \qquad (7)$$

Species richness, *s*, was the total number of species present and *p* was the proportion of the cells of any species *i* to the total number of cells present. Relative diversity values were calculated using the average diversity of the last 1000 days of model simulations divided by the initial diversity. Relative population density values were similarly calculated using the average population density of the last 1000 days divided by the initial population density.

The assemblage resistance is given by the slopes of the boundary between allelopathic monoculture to a multispecies assemblage in the biodiversity maps (in early explorations of the model I discovered this transition to be abrupt, as I will show in the figures). The slope values

were calculated by averaging the changes in ε_c over the changes in KI along the bloom transition boundary, reflecting a shift from the monoculture to a multispecies assemblage.

One way to characterize the competitive power of resource exploitation between species within an assemblage is through evaluation of the distance between species-specific R* values through the three-dimensional resource trade-off space (Roelke and Spatharis 2015). Here, I take that approach further by characterizing the competitive similarity of the allelopathic species to all other members of the assemblage. For this, the three-dimensional distance between each species and the allelopathic species was calculated using the Pythagorean Theorem and orthogonal triangles. So, for a 5-species assemblage there would be 4 distances calculated, for a 6-species assemblage there would be 5 distances calculated, and so on. These distances were averaged, giving one value for each assemblage. I now refer to this calculation as the *allelopathy R* composite distance.*

An emergent behavior of the model is then explored by plotting the *allelopathy R* composite distance* for each of the assemblages against the resistance of each assemblage to allelopathy. In this way, I wase able to explore theoretical relationships between assemblage types (i.e., neutral, lumpy and intransitive) and allelopathy functioning.

Results

Expectantly, population dynamics and assemblage composition changed with increasing effect of allelopathy. For assemblages characteristic of neutrality and lumpy coexistence, assemblages asymptotically approached a species-rich steady state when allelopathic effects were low, and these assemblages included the allelopathic species (representative simulation

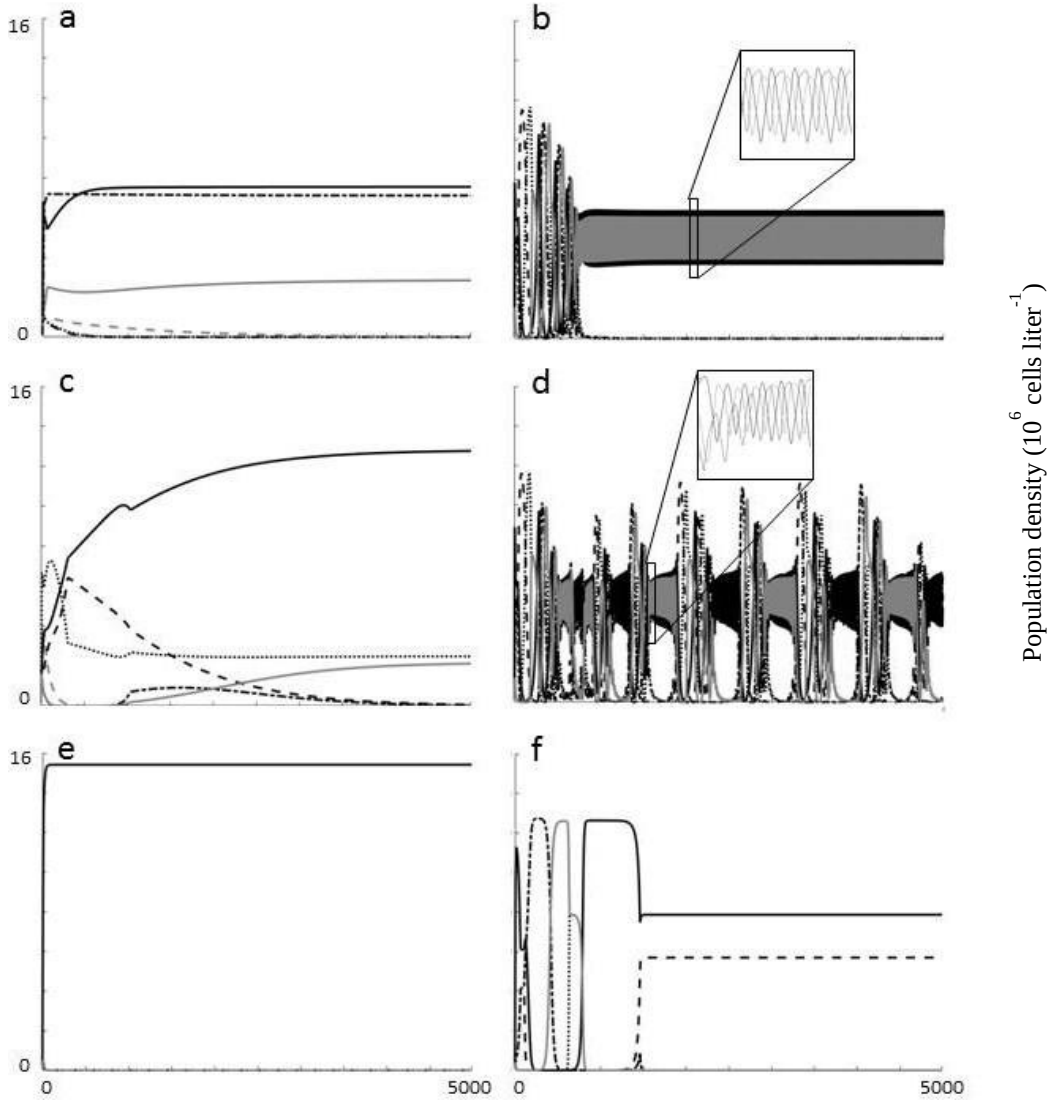

Fiure 2.3. Representative simulations showing population dynamics with different levels of allelopathic influence. Species coexistence for neutral and lumpy assemblages occurred under low (a) and intermediate (c) allelopathic influence, with monospecific blooms occurring under high allelopathic influence (e). Intransitive assemblages of low (b) and intermediate (d) allelopathic influence show coexistence of most species in an oscillating state. But at high allelopathic influence monospecific blooms occur (not shown, but similar to panel e) most of the time, though on occasion, another species coexisted at lower density with the allelopathic species (f). In all panels, the allelopathic species is represented with the solid black line.

shown in Figure 2.3a). As the allelopathic effect increased (either by decreasing KI or increasing ε_c), the allelopathc species increased in dominance (see Figure 2.3c), until eventually high

allelopathic effects led to monospecific blooms of the allelopathic species (see Figure 2.3e). For assemblages characteristic of intransitivity, oscillating and out-of-phase population dynamics resulted when allelopathic effects were low, where the assemblages were comprised of three species (see Figure 2.3b). With an allelopathic effect, sometimes a condition of

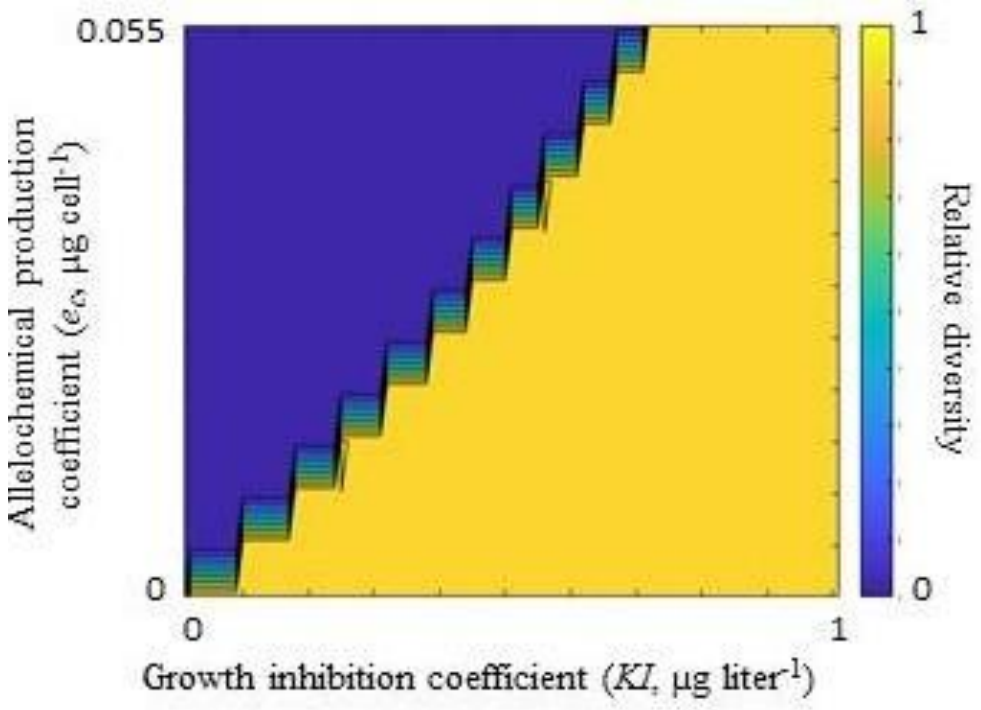

Figure 2.4. The dark blue area indicates combinations of growth inhibition and production resulting in a monospecific bloom of the allelopathic species. The yellow area indicates combinations where the resulting diversity of the assemblage is the same as it was under the initial condition, i.e., no loss of diversity. The slope of the transition boundary between blue and yellow areas, therefore, provides information on the assemblages' resistance to allelochemical effects, where greater slopes reflect greater resistance.

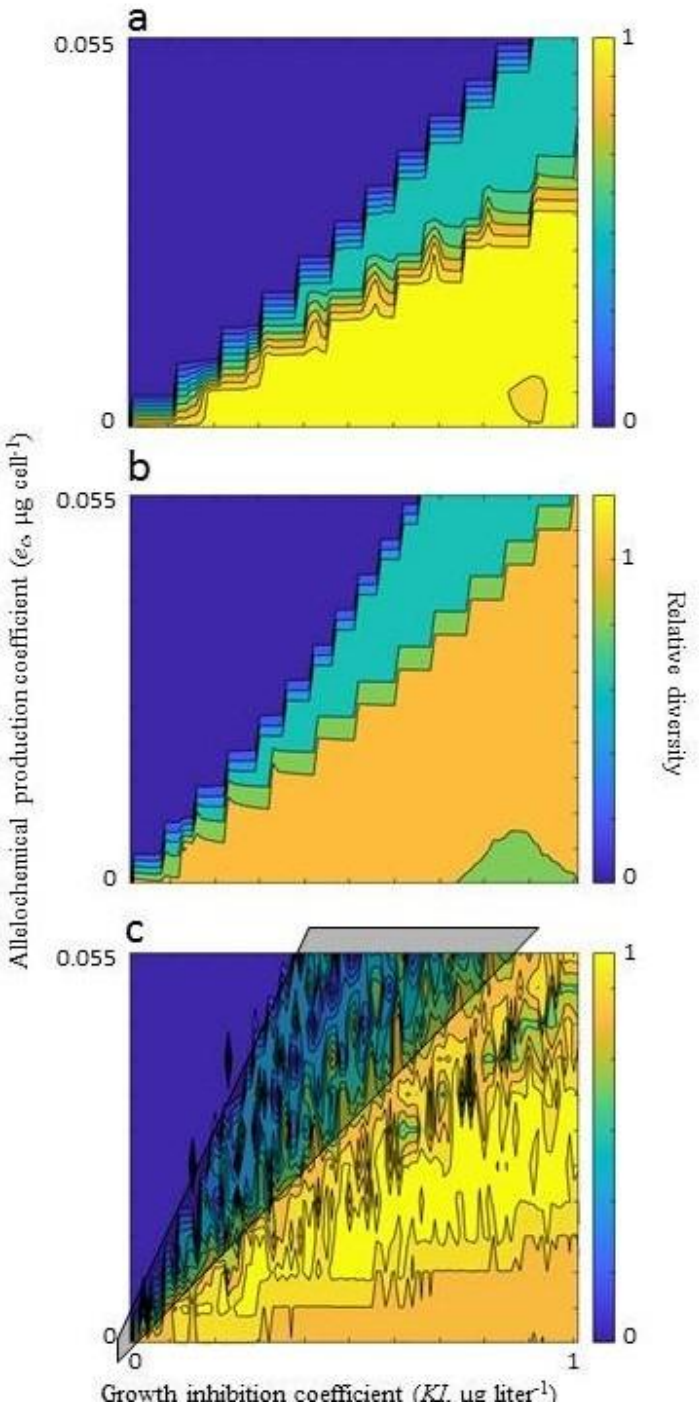

Figure 2.5. Representative diversity maps for neutral (a), lumpy (b) and intransitive (c) assemblages. Neutral diversity maps show the lowest slopes of the first transition boundary (across which monospecific blooms occur), lumpy diversity maps show steeper slopes, and intransitive diversity maps show the steepest slopes. Collapses in relative diversity that occurred in intransitive assemblages in regions of the biodiversity maps to the right of the transition boundaries were not associated with emergence of the allelochemical producing species (c, area under transparent triangle).

alternating states emerged where the assemblages were comprised of five species oscillating and out-of-phase (see Figure 2.3d) or sometimes a steady-state emerged with co-existence of the allelopathic species with another species (see Figure 2.3f). But as the allelopathy effect increased further, a monospecific bloom always resulted (not shown).

Biodiversity maps were all similar in that they showed a trend of high relative diversity rapidly transitioning to low relative diversity (monospecific bloom of the allelopathic species) as allelopathic effects increased (Figure 2.4). They differed, however, in regards to the positioning of this transition boundary along the allelochemical production and competitor sensitivity gradients. Because the transition boundaries were mostly linear over the range of ε_c and KI values explored here, the differing positions of the transition boundaries between assemblages could be quantified based on their slopes. This enabled a comparison between assemblages characteristic of neutrality, lumpy coexistence and intransitivity.

Neutral assemblages had low transitional boundary slopes indicating a low resistance to allelopathy (representative assemblage shown in Figure 2.5a). Lumpy assemblage maps had steeper bloom transition slopes than neutral maps, indicating greater resistance to allelopathic effects than neutral assemblages (Figure 2.5b). Both neutral and lumpy assemblages always showed a unidirectional change from high diversity to low diversity as allelopathic effect increased. Intransitive assemblages showed the steepest slopes of the bloom transition boundaries, indicating even greater resistance to allelopathic effect. With these assemblages, however, the change from high to low relative diversity as allelopathic influence increased was not unidirectional, as relative diversity values sometimes increased with strengthening allelopathic effect (Figure 2.5c). With intransitive assemblages, collapses in relative diversity that occurred in regions

of the biodiversity maps to the right of the monospecific bloom transition boundaries were not always associated with emergence of the allelochemical producing species (shaded region in Figure 2.5c).

As described before, distributions of R* values through the three-dimensional resource trade-off space varied for each assemblage type (Figure 2.2). Having similar R* values for all

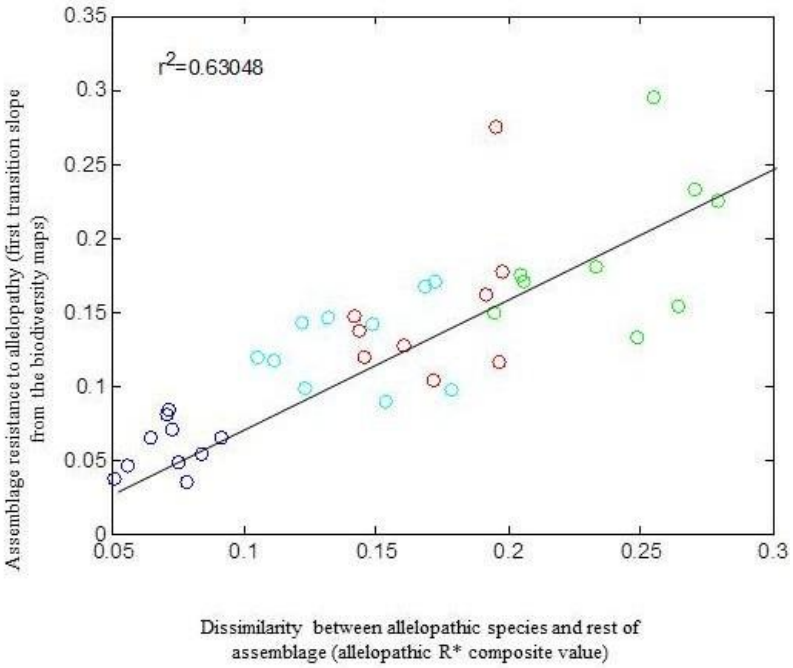

Figure 2.6. A positive correlation exists between an assemblage's ability to resist a monospecific bloom of the allelopathic species (y-axis) and the combined ability of assemblage members to compete for resources under allelopathic influence (x-axis). A near-consistent ranking emerged going from neutral (blue circles), to lumpy (cyan circles), to intransitive assemblages with centrally located allelopathic species (red circles) and finally to intransitive assemblages with peripherally located allelopathic species (green circles).

three resources (i.e., being competitively similar), neutral assemblages occupied a small volume of the resource trade-off space, with species being tightly clustered together (Figure 2.2a). Lumpy assemblages had a wider range of R* values and subsequently occupied a larger volume

of the resource trade-off space (Figure 2.2b), which indicated that the competitive abilities among those assemblages differed more than in neutral assemblages. Species in intransitive assemblages covered the largest volume of the resource trade-off space, having the largest variation in R* values. This indicated that the species in these assemblages were the most competitively dissimilar (Figure 2.2c).

My characterization of resistance to allelopathy, based on the slope of the bloom transition boundary, was positively correlated ($r^2 = 0.63$) to the *allelopathic R* composite distance*, the average distance between all non-allelopathic species of the assemblage and the allelopathic species (Figure 2.6). This relationship was observed within and across assemblage type. Neutral assemblages fared worst in this regard with allelopathic influence, followed by lumpy assemblages, then by intransitive assemblages where the allelopathic species was centrally-located among competitor's R*s, and finally by intransitive assemblages where the allelopathic species was peripherally-located with competitor's R*s.

Discussion

In this model, transitions were abrupt between non-bloom states of higher biodiversity and monospecific bloom states of the allelopathic species. The bloom states were monospecific because of the suppressing effect by interference competition from the allelopathic species on exploitative competition. The transitions were abrupt because of the positive feedback resulting from increased toxin concentration by increasing densities of the allelopathic species, leading to a stronger suppression of their non-allelopathic competitors and a further reduced exploitative competitive effect by the non-allelopathic species. Positive feedbacks leading to rapid bloom formation, such as this, have been surmised from field observations and experiments (Sunda et al. 2006; Granéli et al. 2012). In addition, near-monospecific blooms are commonly observed in

nature (Keating 1978; Michaloudi et al. 2009; Hattenrath-Lehmann et al. 2011). Through my modeling here, I mechanistically demonstrate the functioning of one such positive feedback.

The emergent behavior of this model suggests that an assemblage's resistance to monospecific bloom formation of the allelopathic species may be tied to the degree of competitive interactions between assemblage members. The competitive power of an assemblage is reflected by the distances between extremes of the R* values of species in the resource tradeoff space. In my simulations, the more dissimilar assemblage members were from the allelopathic species in their ability to exploit resources, the more resistant the assemblages became to monospecific blooms of the allelopathic species. In other words, stronger allelochemical effects (through ε_c and KI) were required to overcome assemblages with greater competitive power. This observation of the model's emergent behavior is similar to what has been observed in plant systems that have experienced invasions, where invasion success and impact on residents were a function of the invader's life history traits relative to the life history traits of the residents (Von Holle et al. 2003; Ortega & Pearson 2005; Gruntman et al. 2014).

For some simulations, assemblage states other than the dichotomous biodiverse and monospecific bloom states occurred. Specifically, for some of the intransitive assemblages non-allelopathic species with dissimilar traits from the allelopathic species were able to survive in monoculture or persist with the allelopathic species under high allelopathic effect. In these instances, the population losses arising from allelochemical exposure did not completely mask the advantage gained by being competitively dissimilar. Though the combinations of ε_c and KI where this was observed were few, it occurred several times for some intransitive assemblages. Perhaps this is why sometimes near-monospecific blooms of allelopathic species are observed in nature, as referenced above, and other times non allelopathic species are able to co-exist with

allelopathic species during blooms (Redlaje 2003; Lindholm et al. 1999; West et al. 1996; Figueiredo et al. 2006).

Model results also showed that the incidence of monospecific bloom of the allelopathic species was a function of the assemblage type. For example, neutral assemblages occupied the smallest volume of the three-dimensional resource tradeoff space. Consequently, these allelopathic R* composite distances were the least. The neutral assemblages were also the most vulnerable to monospecific blooms of the allelopathic species. An explanation for this may be that an allelopathic species can be expected to affect the population dynamics of all functionally equivalent members in the same way. So, if we see a negative effect on one species' population, we can expect a similar effect on others as well. Conversely, assemblages characteristic of lumpy coexistence and intransitivity occupied larger volumes of the three-dimensional resource tradeoff space, had greater allelopathic R* composite distances and exhibited stronger resistance to monospecific blooms of the allelopathic species. An explanation for this may be that an allelopathic species can be expected to affect the population dynamics of assemblage members differentially when they are competitively dissimilar. In these scenarios, the magnitude of the negative effect on one species' population would not be expected to be the same on other members. Interestingly, other modeling studies comparing the resistance and resilience of neutral, lumpy and intransitive assemblages to various other processes common in aquatic environments showed that intransitive assemblages were generally much more vulnerable to biodiversity collapses than neutral and lumpy assemblages, suggesting incidence of intransitivity in plankton systems might be rare (Roelke and Eldridge 2008; Bhattacharyya et al. 2018; Withrow et al. 2018). Here, I show that when allelopathic interactions are considered,

intransitive assemblages are more resistant, which suggests intransitivity in plankton systems might not be as rare as previously suggested.

Central to niche theory is the idea that tradeoffs in competitive abilities for multiple resources promotes coexistence among species, a cornerstone of widely embraced theory of resource competition (Tilman 1982). I showed that the relative magnitude of the tradeoffs may lead to differential effects of exploitative and interference competition on individual species. Even small changes in the R* values can strongly influence fitness of assemblage members confronted with allelopathy. This modelling demonstrates that the competitive power of phytoplankton assemblages can influence their resistance to allelopathic blooms. Thus, in aquatic systems, ecosystem stability may be directly linked to differences in exploitative abilities of species at the lowest trophic level.

References

Bhattacharyya, J., D.L. Roelke, R.M.W. Muhl, F.G. Withrow. 2018. Exploitative competition of invaders differentially influences the diversity of neutral, lumpy and intransitive phytoplankton assemblages in spatially heterogeneous environments. Ecological Modelling. 370(C), 59-66.

Buss, L.W. and J.B.C. Jackson. 1979. Competitive networks: nontransitive competitive relationships in cryptic coral reef environments. The American Naturalist. 113(2): 223-234.

Caron D.A., Lim E.L., Kunze H., Cosper E.M., Anderson D.M. 1989.Trophic Interactions Between Nano- and Microzooplankton and the "Brown Tide". In: Cosper E.M., Bricelj V.M., Carpenter E.J. (eds) Novel Phytoplankton Blooms. Coastal and Estuarine Studies (formerly Lecture Notes on Coastal and Estuarine Studies), vol 35. Springer, Berlin, Heidelberg.

Case, T.J. and M.E. Gilpin, 1974. Interference Competition and Niche Theory. Proceedings of the National Academy of Sciences of the United States of America. 71 (8): 3073-3077.

Chase, J.M., M.A. Leibold. Ecological Niches: Linking Classical and Contemporary Approaches. Interspecific Interactions. Chicago (Illinois): University of Chicago Press. 212 pgs.

Chesson, P.L. and R.R. Warner. 1981. Environmental Variability Promotes Coexistence in Lottery Competitive Systems. The American Naturalist. 117(6): 923-943.

Chust, G., Irigoien, X., Chave, J., & Harris, R. 2013. Latitudinal phytoplankton distribution and the neutral theory of biodiversity. Global Ecology and Biogeography. 22: 531-543.

Czaran, T., R.F. Hoekstra and L. Pagie. 2002. Chemical Warfare between Microbes Promotes Biodiversity. Proceedings of the National Academy of Sciences of the United States of America. 99(2): 786-790.

Drost, M. B., Cuppen, H. P., Van Nieukerken, E. J., & Schreijer, M. 1992. De Waterkevers van Nederland. Utrecht, The Netherlands: Uitgeverij.

Durrett, R. and S. Levin. 1997. Allelopathy in Spatially Distributed populations. Journal of Theoretical Biology. 185: 165-171.

de Figueiredo, D.R., A.S.S.P. Reboleira, S.C. Antunes, N. Abrantes, U. Azeiteiro, F. Gonsalves & M.J. Pereira.2006. The effect of environmental parameters and cyanobacterial blooms on phytoplankton dynamics of a Portuguese temperate lake. Hydrobiologia. 568:145–157. doi 10.1007/s10750-006-0196y.

Fistarol, G.O., Legrand, C., and Grane´li, E., 2003. Allelopathic effect of Prymnesium parvum on a natural plankton community. Marine Ecology Progress Series 255, 115–125.

Fort H., M. Scheffer M, E.H. Van Nes. 2010. The clumping transition in niche competition: A robust critical phenomenon. J. Stat. Mech. Article P05005.

Fortner A.M., Weltzin, J.F. 2007. Competitive hierarchy for four common old-field plant species depends on resource identity and availability. J Torrey Bot Soc. 134, 166-176.

Frean, M. and E. R. Abraham. 2001. Rock-paper-scissors and the survival of the weakest. Proc. R. Soc. Lond. B 268: 1323-1327.

Gilpin, M. E. 1975. Limit cycles in competition communities. American Naturalist. 109:51–60.

Granéli, E., B. Edvardsen, D.L. Roelke, J.A. Hagström. 2012. The ecophysiology and bloom dynamics of *Prymnesium* spp. Harmful Algae. 14: 260-270.

Grover, J.P. 1997. Resource Competition. London, Chapman and Hall.

Grover, J., Crane, K., Baker, J., Brooks, B. and Roelke, D. 2010. Spatial variation of harmful algae and their toxins in flowing-water habitats: a theoretical exploration. Journal of Plankton Research.33:2, 211–227.

Gruntman, M., A.K. Pehl, S. Joshi, K. Tielborger. 2014. Competitive dominance of the invasive plant Impatiens glandulifera: using competitive effect and response with a vigorous neighbor. Biol. Invasions. 16: 141–151.

Hattenrath-Lehmann, T.K., C.J. Gobler. 2011. Allelopathic inhibition of competing phytoplankton by North American strains of the toxic dinoflagellate, *Alexandrium fundyense*: Evidence from field experiments, laboratory experiments, and bloom events Harmful Algae 11, 106–116

Havlicek, T.D. and Carpenter, S.R. 2001. Pelagic species size distributions in lakes: are they discontinuous? Limnol. Oceanogr. 46: 1021–1033.

Holling, C. S. 1992. Cross-scale morphology, geometry, and dynamics of ecosystems. Ecol. Monogr. 62: 447–502.

Hubbell, S.P. 2005. The neutral theory of biodiversity and biogeography and Stephen Jay Gould. Paleobiology.31: 122–132.

Huisman, J. and F.J. Weissing. 1999. Biodiversity of plankton by species oscillations and chaos. Nature. 402: 407-410.

Huisman, J. and F.J. Weissing. 2001. Biological conditions for oscillations and chaos generated by multispecies competition. Ecology. 82:2682–2695.

Huisman, J., B. Sommeijer. 2002. Population dynamics of sinking phytoplankton in light-limited environments: simulation techniques and critical parameters. Journal of Sea Research. 48: 83– 96.

Jonsson, P.R., H. Pavia, and G. Toth. 2009. Formation of harmful algal blooms cannot be explained by allelopathic interactions. Proceedings of the National Academy of Sciences of the United States of America. 106: 11177–11182.

Jöhnk, K.D., J. Huisman, J. Sharples, B. Sommeijer, P.M. Visser, J.M. Stroom. 2008. Summer heatwaves promote blooms of harmful cyanobacteria. Global Change Biology. 14: 495-512.

Karlson, R. and Jeremy Jackson. 1981. Competitive Networks and Community Structure: A Simulation Study. Ecology. 62:3 670-678.

Keating. K.I. 1978. Blue-green algal inhibition of diatom growth: transition from mesotrophic to eutrophic community structure. Science. 199: 971–973.

Keddy, Paul. 1989. Competition. Population and Community Biology Series, Springer. 6:1, 224 pgs.

Kerr, B., M.A. Riley, M.W. Feldman and B.J.M. Bohannan. 2002. Local dispersal promotes biodiversity in a real-life game of rock-paper- scissors. Nature 418:171–174.

Kubanek, J., Hicks, M. K., Naar, J. et al. (2005) Does the red tide dinoflagellate Karenia brevis use allelopathy to outcompete other phytoplankton? Limnol. Oceanogr., 50, 883–895.

Laird, R. and Brandon S. Schamp, B. 2006. Competitive Intransitivity Promotes Species Coexistence. The American Naturalist. 168:2.

Legrand C, Rengefors K, Fistarol GO, Granéli E (2003) Allelopathy in phytoplankton—biochemical, ecological, and evolutionary aspects. Phycologia 42:406–419

Leon, J. A., and D. B. Tumpson. 1975. Competition between two species for complementary or substitutable resources. Journal of Theoretical Biology 50:185-201.

Lewis, W.M., Jr. 1986. Evolutionary Interpretations of Allelochemical Interactions in Phytoplankton Algae. The American Naturalist. 127(2):184-194.

Lindholm, Tore, Petra Öhman, Katriina Kurki-Helasmo, Brendan Kincaid & Jussi Meriluoto (1999) Toxic algae and fish mortality in a brackish-water lake in Åland, SW Finland, Hydrobiologia 397: 109–120, 1999.

Litchman E, Klausmeier CA, Schofield OM, Falkowski PG. 2007. The role of phytoplankton functional traits in structuring phytoplankton communities: scaling from cellular to ecosystem level. Ecology Letters. 10:1170–81.

Marquet, PA. 2000. Invariants, scaling laws and ecological complexity. Science 289: 1487-1488.

Martines, I., Kojouharov, H., and Grover, J. 2009. A chemostat model of resource competition and allelopathy. Applied Mathematics and Computation. 215, 573–582.

Maury, O., Shin, Y-J., Faugeras, B., Ari, T.B., and Marsac, F. 2007. Modeling environmental effects on the size-structured energy flow through marine ecosystems, Part 2: simulations. Progress in Oceanography doi: 10.1016/j.pocean.2007.05.001

Nakamaru, M and Iwasa, Y. 2000. Competition by Allelopathy Proceeds in Traveling Waves: Colicin-Immune Strain Aids Colicin-Sensitive Strain. Theoretical Population Biology. 57, 131144.

Neisch, M.T., D.L. Roelke, B.W. Brooks, J.P. Grover, & M.P. Masser. 2012. Stimulating effect of Anabaena sp. exudate on Prymnesium parvum. Journal of Phycology 48: 1045-1049.

Ortega, Y.K., D.E. Pearson. 2005. Weak vs. strong invaders of natural plant communities: Assessing invasibility and impact. Ecological Applications. 15: 651-661.

Poulson, K.L., R.D. Sieg, E. K. Prince and J. Kubanek. 2010. Allelopathic compounds of a red tide dinoflagellate have species-specific and context-dependent impacts on phytoplankton. Mar. Ecol. Prog. Ser. 416: 69–78.

Poulson-Ellestad, K., McMillan, E., Montoya, J., and Kubanek, J. 2014. Are offshore phytoplankton susceptible to Karenia brevis allelopathy? J. Plankton Res. 1–13. doi:10.1093/plankt/fbu064.

Prince, E.K., T.L. Myers, J. Naar and J. Kubanek. 2008. Competing phytoplankton undermines allelopathy of a bloom-forming dinoflagellate. Proc. R. Soc. B 275: 2733–2741. doi:10.1098/rspb.2008.0760.

Redalje, DG, S.E. Lohrenz, M.J. Natter, M.D. Tuel, G.J. Kirkpatrick, D.F. Millie, G.L. Fahnenstiel and F.M. Van Dolah. 2008. The growth dynamics of Karenia brevis within discrete blooms on the West Florida Shelf. Continental Shelf Research. 28: 24–44.

Roelke, D., Augustine, S. and Buyukates, Y. 2003. Fundamental Predictability in Multispecies Competition: The Influence of Large Disturbance. The American Naturalist. 162:5, 615-622.

Roelke, D.L. and P. Eldridge. 2008. Mixing of Supersaturated Assemblages and the Precipitous Loss of Species. Am. Nat. 17(2): 162-175.

Roelke DL, Spatharis S. 2015. Phytoplankton Succession in Recurrently Fluctuating Environments. PLoS ONE 10(3): e0121392.doi:10.1371/journal.pone.0121392.

Sale, P.F. 1977. Maintenance of high diversity in coral reef fish communities. Am. Nat. 111:337-359.

Scheffer, M. and E.H. van Nes. 2006. Self-organized similarity, the evolutionary emergence of groups of similar species. Proceedings of the National Academy of Sciences. 103(16): 620-6235.

Schippers, P., Verschoor, A. M., Vos, M., & Mooij, W. M. 2001. Does "supersaturated coexistence" resolve the "paradox of the plankton"? Ecology Letters. 4: 404-407.

Segura, A.M., D. Calliari, C. Kruk, D. Conde, S. Bonilla, H. Fort. 2011. Emergent neutrality drives phytoplankton species coexistence. Proc. Biol. Sci. 278: 2355–2361.

Segura, A.M., C. Kruk, D. Calliari, F. Garcı´a-Rodriguez, D. Conde, C. E. Widdicombe, H. Fort. 2013. Competition Drives Clumpy Species Coexistence in Estuarine Phytoplankton. Scientific Reports 3: Article Number 1037.

Shannon, C., & Weaver, W. 1949. The Mathematical Theory of Communication. Urbana, IL.: University of Illinois Press.

Sinervo, B., & Lively, C. 1996. The rock-paper-scissors game and the evolution of alternative male strategies. Nature. 380: 240-243.

Smayda, T. J., 1997. What is a bloom? A commentary. Limnology and Oceanography 42(5): 1132–1136.

Sommer, U., Charalampous, E., Genitsaris, S., Moustaka-Gouni, M. 2017. Benefits, costs and taxonomic distribution of marine phytoplankton body size. Journal of Plankton research 39: 494-508.

Suikkanen, S., G.O. Fistarol, E. Granéli. 2005. Effects of cyanobacterial allelochemicals on a natural plankton community. Mar. Ecol. Prog. Ser. 287: 1–9.

Sunda, W.G., E. Graneli, C.J. Gobler. 2006. Positive Feedback and the Development and Persistence of Ecosystem Disruptive Algal Blooms. J. Phycol. 42: 963–974.

Tang, Y.Z. and C. J. Gobler. 2010. Allelopathic effects of Cochlodinium polykrikoides isolates and blooms from the estuaries of Long Island, New York, on co-occurring phytoplankton. 406: 19–31.

Thornton, D.C.O. 2014. Dissolved organic matter (DOM) release by phytoplankton in the contemporary and future ocean. European Journal of Phycology. 49(1): 20-46.

Tilman, D. 1977. Resource competition between planktonic algae: an experimental and theoretical approach. Ecology. 58: 338-348.

Tilman, David. Resource competition and community structure. 1982. Princeton University Press.

Tilman, D. 2004. Niche tradeoffs, neutrality, and community structure: A stochastic theory of resource competition, invasion, and community assembly. Proceedings of the National Academies of Sciences. 101:30, 10854-10861.

Uronen. P., Kuuppo P., Legrand C., and Tamminen T. 2007. Allelopathic effects of toxic haptophyte Prymnesium parvum lead to release of dissolved organic carbon and increase in bacterial biomass. Microbial Ecology. 54:1,183-93.

Von Holle, B., H.R. Delcourt, D. Simberloff. 2003. The importance of biological inertia in plant community resistance to invasion. Journal of Vegetation Science 14: 425-432.

West, T., Marshall, H. G. and Tester, P. A. Natural Phytoplankton Community Responses to a Bloom of the Toxic Dinoflagellate Gymnodinium breve Davis off the North Carolina Coast. Southern Appalachian Botanical Society. 61:4, 356-368.

Withrow, F.G., D.L. Roelke, R.M.W. Muhl, J. Bhattacharyya. 2018. Water column processes differentially influence richness and diversity of neutral, lumpy and intransitive phytoplankton assemblages. Ecological Modelling. 370C: pp. 22-32.

CHAPTER III

TESTING THE ALLELOPATHY MODEL

USING TIME SERIES DATA OF LAKE SYSTEMS

Allocating organisms into size classes has a long history in ecology, and size is among the most important factors in structuring food webs (Maury et al, 2007). Species clustering based on size distribution may be common in nature (Holling 1992; Sakavara et al. 2017) and has been found in freshwater (Drost 1992) and estuarine (Segura et al. 2013) phytoplankton assemblages. Lumpy coexistence describes a condition where traditional niche-based competition and neutral theory are reconciled. In this condition, species self-organize into multiple clusters along resource gradients, in which members of a cluster are competitively neutral and clusters compete for resources (Holling 1992; Scheffer & van Nes 2006; Fort & Scheffer 2010). Phytoplankton cell size is an important feature of ecological function (Litchman and Klausmeier 2008). Predator avoidance (Acevedo-Trejos et al. 2015), the seasonality of temperature (Zohary et al. 2017) and nutrient levels (Acevedo et al. 2015), and resource availability influenced by fluctuating hydrology and consumption patterns (Smeti et al. 2016; Sakavara et al. 2017) all influence the non-random or self-organized size distributions of phytoplankton.

Many factors influence the formation of allelopathic blooms, including trophic state, which I elaborate on here since the lakes in this study have a range of trophic status (discussed below in the Methods). Dense, toxic cyanobacteria blooms of *Anabaena spp*., *Cylindrospermopsis raciborskii*, and *Microcystis spp.* occur readily in eutrophic systems (Keating 1978; Kilham and Kilham 1984; Paerl 1988; Wu et al. 2017). Toxic species in these genera can also thrive and bloom in systems with historically low nutrient levels, including sub-

alpine oligotrophic systems (Salmaso 2000; Callieri et al. 2014) and meso-to eutrophic systems in Canada (Hamilton et al. 2005). Other successful species include the marine dinoflagellate *Karenia brevis*, recognized as a poor competitor for inorganic nutrients, but which is notorious for blooming in coastal areas when nutrient concentrations increase (Steidinger 2009). Alternatively, some species may become better competitors for resources due to increased toxicity in response to a lower nutrient environment (Legrand et al. 2003). For example, the haptophytes *Prymnesium parvum* and *Chrysochromulina polylepis* increase their toxin production under conditions of nitrogen and phosphorous limitation and can form dense toxic blooms as a result (Edvardsen and Paasche 1992; Graneli and Johannson 2003). This variation in effect of nutrients on the allelotoxicity of some species supports the idea that the periodicity and magnitude of nutrient-rich inflows may provide a key to minimizing toxic blooms of some species (Buyukates and Roelke 2001).

Chapter 2 of this dissertation provides support for the idea that the competitive power of an assemblage is a significant factor in an assemblage's ability to resist the effects of allelopathy. In this chapter, the emergent behavior shown by the modelling is tested using phytoplankton time-series data from eight lakes of varied morphometry and trophic state. Most of these lakes have experienced harmful algal blooms at some point in their recent history and the harmful bloom-forming species were known allelochemical producers. To test the idea that the competitive power of an assemblage influences its resistance to allelopathy, I looked for evidence of species clusters (lumps) based on similarity in cellular size in the time-series data, using size distribution of phytoplankton as a proxy for competitive power within assemblages.

Methods

To test whether the emergent behavior observed in the model discussed in chapter 2 could be observed in natural environments, I analyzed multiyear time-series data (ranging from weekly to monthly sampling frequency) of phytoplankton composition and biovolume density from eight freshwater lakes. These were Lake Mikri Prespa (2 ½ years) bordered by Greece and Albania; Lakes Volvi (2 years) and Koronia (1 ½ years) in Greece; Lake Kinneret (19 years) in Israel; Lake Constance (15 years) bordered by Switzerland, Austria and Germany; and Lakes Fancsika 1-es tározó (19 years), Fancsika 2-es tározó (19 years) and Mézeshegyi-tó (19 years) in Hungary. The lakes vary in morphometry and trophic state. Lakes Constance and Kinneret are of large area and greater depth, while being oligotrophic and mesotrophic to eutrophic, respectively. Lakes Volvi and Mikri Prespa are of intermediate area and depth, both being eutrophic. Lakes Fancsika 1-es tározó, Fancsika 2-es tározó and Mézeshegyi-tó are small and shallow, all being eutrophic to hypereutrophic. Lake Koronia is a heavily modified hypereutrophic system that is very large in area and shallow in depth. Details of the collection methods for the eight lakes including sampling and microscopy analyses for cellular size measurements can be found in those studies (Gaedke et al. 1993; Gaedke 1998; Borics et al. 2000, 2013; Michaloudi et al. 2009; Zohary et al. 2012; Moustaka-Gouni et al. 2014). Time-series data for Lakes Mikri Prespa, Volvi, Koronia, and Kinneret included temporal variation in species-specific cellular size. Time-series data for Lakes Fancsika 1-es tározó, Fancsika 2-es tározó, Mézeshegyi-tó and Constance employed an averaged cellular size.

The lake data comprised taxa identified to the species level and cellular size information. The data did not include information on the same life-history traits used in the numerical modeling that defined species competitive abilities (chapter 2). Instead, competitive abilities

within lake assemblages were surmised by us based on the size distribution of phytoplankton species with a specific focus on the incidence and number of co-occurring species clusters (this is explained further below). Insights into mechanisms that link assemblage structure to efficacy of allelopathy were then achieved through comparisons of emergent behavior of the model (from chapter 2) and emergent behavior of the assemblages observed in the lakes.

Time-series data were processed as species-specific biovolume density (μm^3 $liter^{-1}$) and species-specific cellular biovolume (μm^3 $cell^{-1}$). To determine assemblage cellular size distribution for each sampling date, I first $\log_{10}$ transformed cellular biovolume values, then parsed the transformed data into pre-defined size classes. The pre-defined size classes were based on the largest species from all eight lakes and an optimal number of size classes. The number of size classes to be used was identified by exploring multiple pre-defined size classes until a number was found that optimized the tradeoff between the number of size classes and the size range over which each size class spanned. This optimization process resulted in 23 size classes being selected, which spanned the range from the smallest to largest sized taxa found in all eight lakes (Table 3.1). Following this procedure meant that size classes applied to each lake's assemblages were the same, thus enabling a comparison of assemblages across lakes. The results reported here were robust over a large range of predetermined size classes.

To determine the incidence and number of species clusters occurring within assemblages, the number of species occurring within each of the 23 size classes at each sampling date was summed. The presence or absence of a species was registered once, independent of their biovolume density. In other words, size-frequency histograms were created. An algorithm was developed to quantify the number of species clusters for each sampling date using a slope criteria

applied to the size-frequency histograms. The algorithm identified "peaks" in the size-frequency histograms that were only considered as central locations of species clusters if the slope from the

Table 3.1 Size classes and phytoplankton size distribution used for all lake systems.

Table 3.1. Lower and upper cell size (μm^3 $cell^{-1}$) for each of the 23 size classes.				
	Size Class	Lower boundary	Upper boundary	
	1	0.00	1.68	
	2	1.68	2.84	
	3	2.84	4.78	
	4	4.78	8.05	
	5	8.05	13.56	
	6	13.56	22.84	
	7	22.84	38.46	
	8	38.46	64.79	
	9	64.79	109	
	10	109	183	
	11	183	309	
	12	309	521	
	13	521	878	
	14	878	1479	
	15	1479	2491	
	16	2491	4197	
	17	4197	7069	
	18	7069	11907	
	19	11907	20056	
	20	20056	33782	
	21	33782	56902	
	22	56902	95844	
	23	95844	161435	

preceding minima, or "valley" (moving from smaller size taxa to larger) was ≥ 3, and the slope to the following minima, or the next "valley" (still moving from smaller size taxa to larger) was ≤ -3 (Figure 3.1). In this way, the number of central locations of species clusters, or simply the number of species clusters, was identified for each assemblage for each observation period from each lake.

An emergent behavior of these lake systems was then explored. For this, I calculated the average number of species clusters occurring on any given day of sampling in each of the lakes.

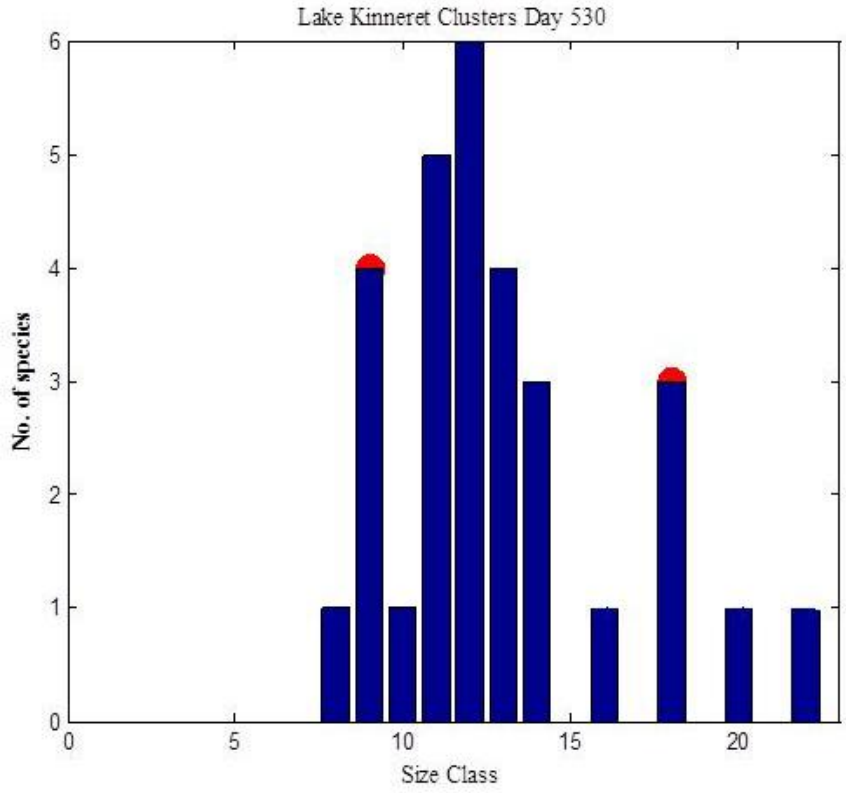

Figure 3.1 Aggregations were identified as clusters if the relationship of species richness and size class fulfilled the slope criteria for a "peak" in a species cluster. Species clusters are noted, with peaks marked with a red solid dot.

I then calculated the average biovolume density of allelopathic bloom-forming taxa occurring during periods when the summed biovolume densities of allelopathic species reached seasonal

peaks. These values were plotted against each other to enable exploration of relationships between assemblage structure (here, the average number of species clusters) and allelopathy functioning (the average magnitude of biovolume density maxima of allelopathic species). For my purposes, species were considered allelopathic only if exogenous toxicity was reported in the literature.

Results

Biovolume density ($\mu m^3 L^{-1}$) of all allelopathic species combined typically showed seasonal maxima (representative example for Lake Fancsika 1-es tározó, Figure 3.2a). The averaged biovolume density of these summed allelopathic species maxima varied between lakes, with Lakes Mézeshegyi-tó, Fancsika 1-es tározó, Koronia and Fancsika 2-es tározó showing the highest values and Lakes Mikri Prespa, Volvi, Kinneret and Constance showing lower values (Table 3.2, Figure 3.3). The size structure of assemblages varied over time, as did the number of species clusters (representative example for Lake Fancsika 1-es tározó, Figure 3.2 middle and bottom panels). The average number of species clusters observed on a sampling day for each lake varied between lakes, with Lakes Mikri Prespa, Kinneret, Volvi and Constance having higher values, followed by Lakes Koronia, Fancsika 1-es tározó, Fancsika 2-es tározó and Mézeshegyi-tó (Table 3.2, Figure 3.3). A negative correlation between the average biovolume density maxima of allelopathic species and the average number of species clusters for each system was observed.

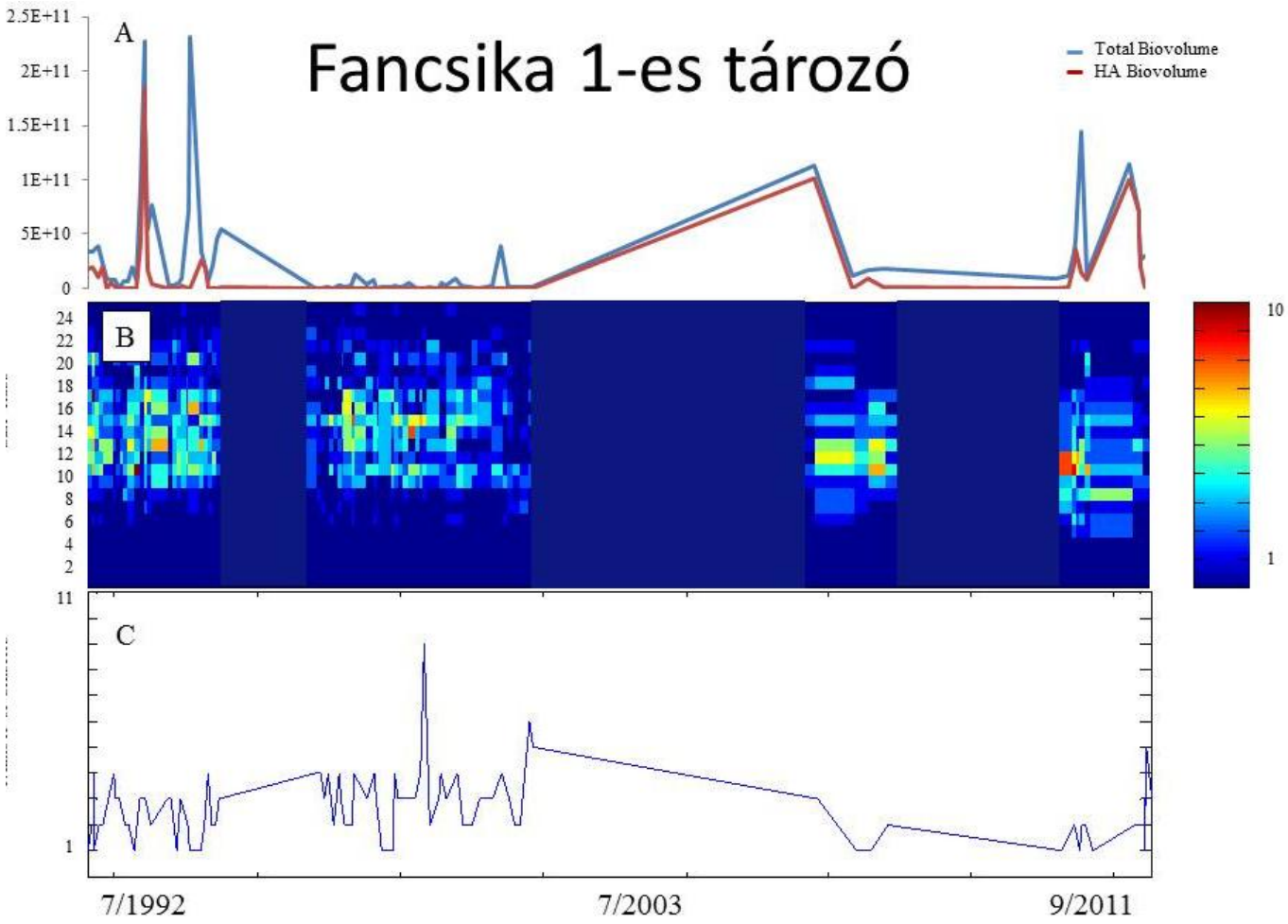

Figure 3.2. Biovolume density over time for total phytoplankton and the sum of all allelopathic taxa (top), the number of taxa occurring in each of the standardized size classes over time (middle), and the average number of species clusters observed over time (bottom).

Table 3.2. Biovolume averages of maxima peaks and average number of clusters for each lake system

Table 3.2 The averages for peak biovolume of allelopathic species and species clusters per lake		
Lake	Average Peak Biovolume of Allelopathic species ($\mu m^3 L^{-1}$)	Average Number Species Clusters
Mézeshegyi-tó	3.22E+11	2.6117
Fancsika 1-es tározó	3.42E+10	2.6548
Koronia	2.29E+10	2.9524
Fancsika 2-es tározó	2.02E+10	2.6118
Mikri Prespa	1.27E+10	4.5135
Volvi	3.24E+09	4.1351
Kinneret	1.11E+09	4.2157
Constance	1.71E+05	4.0419

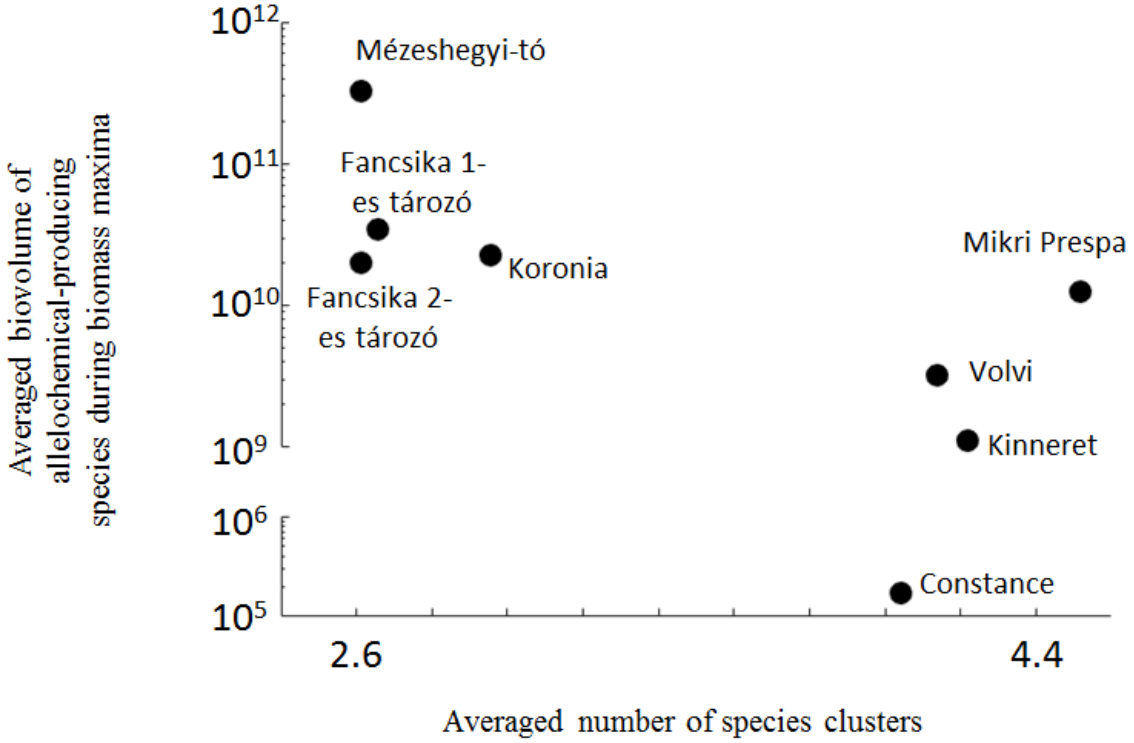

Figure 3.3 There is a negative relationship between average number of species clusters in a system and the peak allelopathy biovolume for a system. Lakes with fewer average species clusters are characterized by higher average peak allelopathic biovolume.

Discussion

The lake systems in this study were lumpy, shown by the distribution of species over the range of size classes, listed in Appendix 4.1 Indeed, phytoplankton systems are characteristically lumpy, a conservative feature apparent in sediment records dating back a few thousand years (Segura et al., 2013). The single most important driver in shaping this distribution may be exploitative competition for resources (Segura et al., 2013). Here, I link this type of competitive interaction to the resistance of an assemblage to allelopathy. Analysis of the time series data in this study shows that a lake's history of allelopathic species dominance (in the extreme, blooms)

is related to the number of species clusters occurring in those lakes, an emergent trend similar to that of my modeling in chapter 2. If we assume that the biovolume density of allelopathic species is, in part, influenced by the resistance of the phytoplankton assemblage to monospecific blooms of allelopathic species (which I show in theory in chapter 2); and if we assume that an assemblage that is characteristic of species clustering is more resistant to allelopathic species than assemblages without species clusters (again, which I show in theory in chapter 2); then an inverse relationship should exist between biovolume density of allelopathic species and species clustering, which is indeed the case with the lakes analyzed here.

A multitude of factors influence phytoplankton assemblage structure and succession. These include the seasonal influences of biotic interactions (Sommer et al 2012), phytoplankton invasion (Hallegraeff 1993; Olenina et al. 2010), environmental disturbance (Connell 1978), and fluctuations in light (Lichtman et al. 2001) and temperature (Rasconi 2017). There is much literature of studies on nutrient flux of a system, for example, through nutrient loading (Roelke 2010), or losses due to biologic activity (McCormack et al. 2015). These events represent system perturbations that do not necessarily create a periodicity in the nutrient regime. In the context of this research, however, it is instructive to discuss fluctuations in resource levels as regular disturbances shaping the distribution and biodiversity of phytoplankton species in an assemblage. There are many factors that contribute to a fluctuating resource environment, which in turn can prevent competitive exclusion and promote biodiversity of phytoplankton assemblages (Roelke and Eldridge, 2008). Some of these factors include mixing (Roelke et al., 1999; Codeco and Grover 2001), influences of seasonal weather patterns (Sommer et al. 1986; Reynolds 1993), and biologic effects of grazing (McCauley and Briand 1979) and pathogens (Brussard 2004), all of which contribute to the resource heterogeneity of a system.

Even at the scale of the assemblage, which this research explores, ecological models show how a fluctuating resource environment can explain the vast biodiversity in phytoplankton assemblages. For example, at the scale of the assemblage, fluctuation in resource levels created by the dynamics of resource competition allows multiple species to coexist (Huisman and Weissing, 1999), and resource fluctuations modeling the seasonal switching of resource supply can create clustering of phytoplankton species (Sakavara et al., 2017), a dynamic that applies to the lakes in my study. The complementarity of an assemblage—the synergistic effect of resource competition among assemblage members that leads to greater resource use--can be affected by the timing of changes in resource supply rate, and a positive relationship exists between the degree of complementarity and species' organization into clusters (Roelke and Spatharis, 2015). Extreme fluctuations that alter the resource levels can reduce biodiversity, but moderate rates of perturbations in the supply rate can maximize the biodiversity of an assemblage (Lubchenco 1978; Tilman 1982)

The lumpiness of an assemblage is but one factor influencing the biovolume density of an allelopathic species in an assemblage, as I suggest here. Other biological processes, such as disruption of grazing (Caron et al.1989) and adaptation to low light environments (Jöhnk et al. 2008), can influence algal bloom density. Nutrient-enriched inflows (Roelke et al. 2010), basin morphometry as it influences mixing depth (Huisman and Sommeijer 2002) and the direct effect of allelopathic compounds (Fistarol et al. 2003) are also important. Here, however, I suggest that an assemblage's resistance to allelopathic species, through the mechanism of exploitative resource competition, is another process influencing algal bloom biomass. Scheffer (2018) suggests that the slow rate of species displacement promotes coexistence (Scheffer 2018). Here I show that magnitude of the competition, ie, the competitive power of an assemblage, is a factor

promoting coexistence among species in clusters with similar species. These findings suggest that an understanding of environmental conditions that structure plankton assemblages, at least in regards to the competitive power of assemblages, is necessary to better understand factors that influence the proliferation of harmful algal blooms.

References

Acevedo-Trejos, E., Gunnar Brandt, Jorn Bruggeman & Agostino Merico. Mechanisms shaping size structure and functional diversity of phytoplankton communities in the ocean Scientific Reports volume 5, Article number: 8918 (2015) doi:10.1038/srep08918.

Borics, G., Grigorszky, I., Szabo, S. and Padisak, J. 2000. Phytoplankton associations in a small hypertrophic fishpond in East Hungary during a change from bottom-up to top-down control. Hydrobiologia. 424: 79–90.

Borics, G., L. Nagy, S. Miron, I. Grigorszky, Z. Laszlo-Nagy, B.A. Lukacs, L. G-Toth, G. Varbıro. 2013. Which factors affect phytoplankton biomass in shallow eutrophic lakes? Hydrobiologia. 714: 93-104.

Brussaard, C. P. D. 2004. Viral control of phytoplankton populations: a review. Journal of Eukaryotic Microbiology 51:125-138.

Caron D.A., Lim E.L., Kunze H., Cosper E.M., Anderson D.M. 1989.Trophic Interactions between Nano- and Microzooplankton and the "Brown Tide". In: Cosper E.M., Bricelj V.M., Carpenter E.J. (eds) Novel Phytoplankton Blooms. Coastal and Estuarine Studies (formerly Lecture Notes on Coastal and Estuarine Studies), vol 35. Springer, Berlin, Heidelberg. America. 99(2): 786-790.

Callieri, C., Roberto Bertoni, Mario Contesini, Filippo Bertoni. 2014. Lake Level Fluctuations Boost Toxic Cyanobacterial "Oligotrophic Blooms". //doi.org/10.1371/journal.pone.0109526

Codeco, C. T., and J. P. Grover. 2001. Competition along a spatial gradient of resource supply: a microbial experimental model. American Naturalist 157:300-315.

Connell, J.H. 1978. Diversity in Tropical Rain Forests and Coral Reefs. Science. 199: 4335,1302-1310.

Drost, M. B., Cuppen, H. P., Van Nieukerken, E. J., & Schreijer, M. 1992. De Waterkevers van Nederland. Utrecht, The Netherlands: Uitgeverij.

Fort H., M. Scheffer M, E.H. Van Nes. 2010. The clumping transition in niche competition: A robust critical phenomenon. J. Stat. Mech. Article P05005.

Edvardsen B, Paasche E (1992) Two motile stages of *Chrysochromulina polylepis* Prymnesiophyceae): morphology, growth and toxicity. J Phycol 28:104–114

Fistarol, G.O., Legrand, C., and Grane´li, E., 2003. Allelopathic effect of Prymnesium parvum on a natural plankton community. Marine Ecology Progress Series 255, 115–125.

Gaedke, U. and Schweizer, A. 1993. Oecologia. The first decade of oligotrophication in Lake Constance. 93: 268.

Gaedke, U. 1998. Functional and taxonomical properties of the phytoplankton community: Interannual variability and response to re-oligotrophication. Arch. Hydrobiol. Spec. Issues: Advances in Limnology 53: 119-141.

Grane´li, E., Johansson, N., 2003. Increase in the production of allelopathic substances by *Prymnesium parvum* cells grown under N- or P-deficient conditions. Harmful Algae 2, 135–145.

Gruntman, M., A.K. Pehl, S. Joshi, K. Tielborger. 2014. Competitive dominance of the invasive plant Impatiens glandulifera: using competitive effect and response with a vigorous neighbor. Biol. Invasions. 16: 141–151.

Hallegraeff, G.M. 1993. Review of harmful algal blooms and their apparent global increase. Phycologia 32:79-99.

Hamilton, P., Ley, L.A., Dean, Stuart, and Pick Frances. 2005. The occurrence of the cyanobacterium Cylindrospermopsis raciborskii in Constance Lake: an exotic cyanoprokaryote new to Canada. Phycologia, 44:1, 17–25.

Havlicek, T.D. and Carpenter, S.R. 2001. Pelagic species size distributions in lakes: are they discontinuous? Limnol. Oceanogr. 46: 1021–1033.

Holling, C. S. 1992. Cross-scale morphology, geometry, and dynamics of ecosystems. Ecol. Monogr. 62: 447–502.

Huisman, J., B. Sommeijer. 2002. Population dynamics of sinking phytoplankton in light-limited environments: simulation techniques and critical parameters. Journal of Sea Research. 48: 83– 96.

Jöhnk, K.D., J. Huisman, J. Sharples, B. Sommeijer, P.M. Visser, J.M. Stroom. 2008. Summer heatwaves promote blooms of harmful cyanobacteria. Global Change Biology. 14: 495-512.

Keating. K.I. 1978. Blue-green algal inhibition of diatom growth: transition from mesotrophic to eutrophic community structure. Science. 199: 971–973.

Kilham, SS and Kilham, P. 1984. The Importance of Resource Supply Rates in Determining Phytoplankton Community Structure, in Trophic interactions within aquatic ecosystems. Eds. Dewey G. Meyers and J. Rudi Strickler.

Legrand C, Rengefors K, Fistarol GO, Granéli E (2003) Allelopathy in phytoplankton—biochemical, ecological, and evolutionary aspects. Phycologia 42:406–419

Litchman E, Klausmeier CA. 2001. Competition of phytoplankton under fluctuating light. Am. Nat. 157:170– 87.

Litchman E, Klausmeier CA, Schofield OM, Falkowski PG. 2007. The role of phytoplankton functional traits in structuring phytoplankton communities: scaling from cellular to ecosystem level. Ecology Letters. 10:1170–81.

Lubchenco, J., and B. A. Menge. 1978. Community development and persistence in a low rocky intertidal zone. Ecological Monographs 48:67-94.

Marquet, PA. 2000. Invariants, scaling laws and ecological complexity. Science 289: 1487-1488.

Maury, O., Shin, Y-J., Faugeras, B., Ari, T.B., and Marsac, F. 2007. Modeling environmental effects on the size-structured energy flow through marine ecosystems, Part 2: simulations. Progress in Oceanography doi: 10.1016/j.pocean.2007.05.001

McCauley, E., and F. Briand. 1979. Zooplankton grazing and phytoplankton species richness: field tests of the predation hypothesis. Limnology and Oceanography 24:243-252.

Michaloudi, E., M. Moustaka-Gouni, S. Gkelis, & K. Pantelidakis. 2009. Plankton community structure during an 886 ecosystem disruptive algal bloom of Prymnesium parvum. Journal of Plankton Research 31: 301-309.

Moustaka-Gouni, M., Michaloudi, E., Sommer, U. 2014. Modifying the PEG model for Mediterranean lakes - no biological winter and strong fish predation. Freshwater Biology 59: 1136-1144.

Olenina, Irina, Norbert Wasmund, Susanna Hajdu, Iveta Jurgensone, Sławomira Gromisz, Janina Kownacka, Kaire Toming, Diana Vaiciute, Sergej Olenin. 2010. Assessing impacts of invasive phytoplankton: The Baltic Sea case. Marine Pollution Bulletin 60, 1691–1700.

Paerl, H.W. 1988. Nuisance phytoplankton blooms in coastal, estuarine,and inland waters. Limnol. Oceanogr., 33(4, part 2) 823-847.

Rasconi, S., Katharina Winter, and Martin J. Kainz. 2017. Temperature increase and fluctuation induce phytoplankton biodiversity loss – Evidence from a multi-seasonal mesocosm experiment. Ecol Evol. 2017 May; 7(9): 2936–2946.

Reynolds, C. S. 1993. Scales of disturbance and their role in plankton ecology. Hydrobiologia 249:157-171.

Roelke, D. L., P. M. Eldridge, and L. A. Cifuentes. 1999. A model of phytoplankton competition for limiting and nonlimiting nutrients: implications for development of estuarine and nearshore management schemes. Estuaries 22:92-104.

Roelke, D. L., and Y. Buyukates. 2001. The diversity of harmful algal bloom-triggering mechanisms and the complexity of bloom initiation. Human and Ecological Risk Assessment 7:1347-1362.

Roelke, D.L., Eldridge, P.M., 2008. Mixing of supersaturated assemblages and the precipitous loss of species. Am. Nat. 171, 162–175.

Roelke, D. and Eldridge, P. 2010. Losers in the 'Rock-Paper-Scissors' game: The role of non-hierarchicalcompetition and chaos as biodiversity sustaining agents in aquatic systems. Ecological Modelling, 221, 1017–1027.

Roelke D., Spatharis S. 2015. Phytoplankton Succession in Recurrently Fluctuating Environments. PLoS ONE 10(3): e0121392.doi:10.1371/journal.pone.0121392.

Salmaso, N. 2000. Factors affecting the seasonality and distribution of cyanobacteria and chlorophytes: a case study from the large lakes south of the Alps, with special reference to Lake Garda. Hydrobiologia, Volume 438, Issue 1–3, pp 43–63. https://doi.org/10.1023/A:1004157828049

Sakavara, A., George Tsirtsis, Daniel L. Roelke, Rebecca Mancy, Sofie Spatharis 2017. Lumpy coexistence under fluctuating resources. Proceedings of the National Academy of Sciences. DOI: 201705944; DOI: 10.1073/pnas.1705944115

Scheffer, M. and E.H. van Nes. 2006. Self-organized similarity, the evolutionary emergence of groups of similar species. Proceedings of the National Academy of Sciences. 103(16): 620-6235.

Scheffer, Martine, Egbert H. van Nes , and Remi Vergnon. 2018. Toward a unifying theory of biodiversity. PNAS. 115: 4, 639–641.

Segura, A.M., D. Calliari, C. Kruk, D. Conde, S. Bonilla, H. Fort. 2011. Emergent neutrality drives phytoplankton species coexistence. Proc. Biol. Sci. 278: 2355–2361.

Segura, A.M., C. Kruk, D. Calliari, F. Garcı´a-Rodriguez, D. Conde, C. E. Widdicombe, H. Fort. 2013. Competition Drives Clumpy Species Coexistence in Estuarine Phytoplankton. Scientific Reports 3: Article Number 1037.

Smeti, E., Roelke, D. and Spatharis, S. 2016. Spatial averaging and disturbance lead to high productivity in aquatic metacommunities. Oikos 125: 812–820.

Sommer, U., Z. M. Gliwicz, W. Lampert, and A. Duncan. 1986. The PEG model of seasonal succession of plankton events in freshwaters. Archiv fir Hydrobiologie 106:436-440.

Sommer, Ulrich, Adrian, R. De Senerpont Domis, L., Elser, J., Gaedke, U., Ibelings, B., Jeppesen, E., Lürling, M., Molinero, J., Mooij, W., van Donk, E., and Winder, M. 2012. Beyond the Plankton Ecology Group (PEG) Model: Mechanisms Driving Plankton Succession Annual Review of Ecology, Evolution, and Systematics. 43:429-448.

Sommer, U., Charalampous, E., Genitsaris, S., Moustaka-Gouni, M. 2017. Benefits, costs and taxonomic distribution of marine phytoplankton body size. Journal of Plankton research 39: 494-508.

Steidinger, K.A. 2009. Historical perspective on Karenia brevis red tide research in the Gulf of Mexico. Harmful Algae 8(4):549-561.

Sunda, W.G., E. Graneli, C.J. Gobler. 2006. Positive Feedback and the Development and Persistence of Ecosystem Disruptive Algal Blooms. J. Phycol. 42: 963–974.

Tilman, D. 1977. Resource competition between planktonic algae: an experimental and theoretical approach. Ecology. 58: 338-348.

Tilman, David. Resource competition and community structure. 1982. Princeton University Press.

Von Holle, B., H.R. Delcourt, D. Simberloff. 2003. The importance of biological inertia in plant community resistance to invasion. Journal of Vegetation Science 14: 425-432.

Wu, Y., Tang, J., Lui, J., Graham, B., Kerr, P. and Chen, H. 2017. Sustained high nutrient supply as an allelopathic trigger between periphytic biofilm and *Microcystis aeruginosa.* Environ. Sci. Technol.,DOI: 10.1021/acs.est.7b01027.

Zohary, T., Nishri, A., and Sukenik, A. 2012. Present–absent: a chronicle of the dinoflagellate *Peridinium gatunense* from Lake Kinneret. Hydrobiologia. 698:161–174.

CHAPTER IV

FIELD EXPERIMENTS IN GALVESTON AND MATAGORDA BAYS

First documented in the United States in Texas in the early 1980s, the invasive toxic haptophyte *Prymnesium parvum* (Carter, 1937) is widespread in the United States and has been found in all coastal states (James and De La Cruz, 1989; Sager et al., 2008). Blooms of *P. parvum* occur with regularity in Texas lakes in the winter, particularly in the Colorado and Brazos river watersheds. The success of this species is due in great measure to its allelopathic capability (Lindholm 1999; Graneli and Johansson 2003). It characteristically releases chemical compounds that kill or reduce the growth of other phytoplankton (Legrand et al. 2003), but its negative effects on plankton (Schwierzke et al., 2010) and fish (Southard et al., 2010; Van Landeghem et al, 2013) are well known. It often creates blooms in which it dominates other species and can contribute a large percentage of total biomass (Fistarol 2003). Millions of fish in Texas reservoirs on the Brazos and Colorado Rivers have died from the ichthyotoxic effects of *P. parvum* (Southard et al., 2010). The Colorado River has experienced the loss of channel catfish (*Ictalurus punctatus*) in some of its reservoirs, with other species decreasing in both rivers (VanLandeghem et al., 2013).

The efficacy of allelochemicals in phytoplankton species is linked to a myriad of factors. Water nutrient levels (Roelke et al., 2007; Graneli and Salomon, 2010), salinity (Baker et al., 2007), irradiance (Fiori et al., 2012) and temperature (Larsen et al., 1993; Baker et al., 2007) are all known to affect *P. parvum* toxicity and allelopathy. Another influence on *P. parvum* is pH. Reduced toxicity of *P. parvum* associated with lower pH has long been known in marine and estuarine systems (Shilo and Aschner, 1953; Ulitzur and Shilo, 1964), and has been associated more recently in freshwater systems in Texas (Prosser et al., 2012). Valenti et al. (2010)

conducted field experiments and found that *P. parvum* toxicity greatly increased between experimental treatments of pH 7.5 and 8.5. Based on this, they proposed that at higher pH, a larger proportion of *P. parvum* toxins prymensin-1 and prymnesin-2 are unionized, facilitating transfer across cellular membranes and causing harm (Valenti et al. 2010). A complete loss of toxicity may be difficult to attain in *P. parvum*, or is at least below ecologically-relevant levels in freshwater and marine systems. Early lab experiments demonstrated near-elimination of toxicity below 6.5 pH (McLaughlin 1958), with similar findings in a freshwater reservoir in Texas (Southard and Klein 2005). Even with a reduction in toxicity, *P. parvum* cells persisted in low pH treatments after 24 hours (Southard and Klein 2005).

Optimum growth of *P. parvum* occurs in salinity and temperature ranges typical of Texas estuarine environments in the summer and fall (Baker et. al 2007). However, with the occurrence of wintertime conditions, those systems may become favorable for an increase in *P. parvum* toxicity as seasonal conditions of low light, low temperature and limited nutrients develop (Fiori et al., 2012; Baker et al., 2007; Liu et al., 2015, Roelke et al., 2007). Occasionally, *P. parvum* has been identified in fringing habitats of the Galveston Bay system, with a suspected bloom in 2005 (Southard et al., 2010; Nelson and Byrd 2011; Roelke et al. 2011). To the west, a *P. parvum* bloom was confirmed in late 2013 in the northern part of East Matagorda Bay system by a Texas Parks and Wildlife (TWPD) research team.

A *P. parvum* bloom in either bay would further stress already vulnerable coastal systems. In the recent past, for example, all Upper Gulf Coast bay systems were closed for fishing due to a sustained bloom of another toxic species, *Karenia brevis*, the effects of which were likely compounded by the extreme drought preceding the bloom. The economic damage of *P. parvum* blooms in Texas is high, and is currently limited to freshwater systems. In 2001, the year of the

first major *P. parvum* bloom in Texas, fish hatcheries along the Brazos River were decimated several years in a row, and in the decade following, economic losses to the state were in the tens of millions of dollars (Southard et al., 2010). Preserving the health and productivity of Texas estuaries is paramount in the face of the threat a toxic *P. parvum* bloom poses, even as increasing human pressures risks their ecosystem functioning and ecosystem services. The Matagorda Bay system is situated between the termination of the Brazos and Colorado rivers, and may accrue a higher risk of *P. parvum* abundance as a result. Galveston Bay has one of the most productive network of fisheries globally, so a bloom of *P. parvum* would be devastating there.

The historical average monthly pH in Galveston Bay is 7.7 and the average monthly pH in Matagorda Bay is above 8.0 (TCEQ, 1986-2013; Criner and Johnican, 2001; Hu et al., 2015). Levels in pH differ naturally in part due to differences in the geologic character of the drainage basins for each bay system. Matagorda Bay has twice the average $CaCO_3$ concentration that the Galveston Bay system has, 269 mg/L and 113mg/L, respectively (Anderson and Rodriguez 2008). Upper Carancahua Bay in the Matagorda Bay system had been in remediation for high pH levels for years, and only recently moved out of that status (TCEQ 2006). Both systems experience wide pH fluctuations in any given month. However, the higher annual average pH of the Matagorda Bay system, coupled with its location between the Brazos and Colorado rivers (Figure 4.1), which have experienced frequent and prolonged *P. parvum* blooms, suggests that this bay is likely an area of future *P. parvum* bloom success. Given past findings of *P. parvum* toxicity linked to pH level, I conducted a comparative study and hypothesized that the response of *P. parvum* in pH-manipulated experiments using Matagorda Bay waters would demonstrate greater population growth and overall toxicity than pH-manipulated experiments using Galveston Bay waters. The goal of the present study was to investigate bloom dynamics of *P. parvum* in

estuarine settings, with a focus, in part on pH level (*P. parvum* growth phase and presence of large grazers were also manipulated in a full factorial experimental design, as described below). For this study, I chose three pH levels, ambient (above 8.0 for all four experiments), 7.5 and 7.0. This decision was based in part on previous research in freshwater lakes in Texas that demonstrated differences in *P. parvum* density response to these levels of pH, specifically that a pH of 8.5 is favorable for *P. parvum* bloom formation, and levels under 7.5 can prevent or mitigate bloom formation (Valenti et al. 2010; Prosser et. al 2012). The decision of a comparative study in Texas bay systems was influenced by the success of *P. parvum* in forming blooms in estuarine settings (Graneli et al., 2012). The lowest pH level used here would not have a negative effect on growth of coastal species (Hinga 1992; Nielsen et al., 2012).

Materials and Methods

Site Description

The Galveston Bay (GB) system is located on the upper Texas Coast, one of several bays that comprise the largest estuarine system in the western Gulf of Mexico (Figure 4.1). Local bayous and creeks provide freshwater runoff into GB, with the San Jacinto and the Trinity rivers contributing more than 80% of the freshwater into the bay (Villalon 1998). The Matagorda Bay (MB) system is located about 100 miles south, part of another large system with no connectivity between its east and west sections. Several rivers empty into MB, notably the Colorado and the Lavaca, in addition to many smaller streams. Both systems are remarkably shallow and are classified as eutrophic, and they have an average yearly water temperature range of 9°C in the

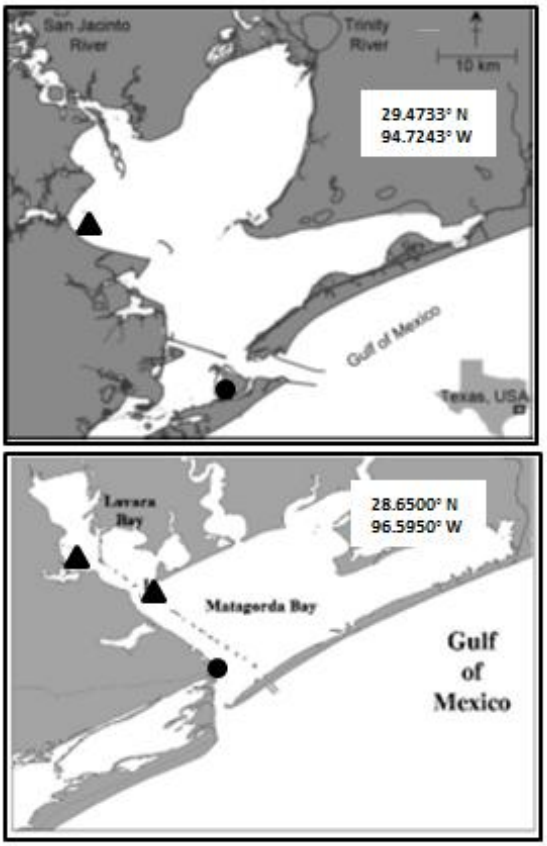

Figure 4.1. Galveston (top) and Matagorda bays (bottom). Filled stars indicate where water was collected, and filled squares show where experiments were deployed (Top panel adapted from Lundgren et al. 2015).

winter to 34°C in late summer (CCMA-NOAA). They have limited exchange with oceanic waters and are partially enclosed by a series of barrier islands. Nutrient levels in the bays fluctuate seasonally and are tied to freshwater inflows, with nutrients generally low in late summer and higher in early spring. The waters in both systems sometimes experience persistently high salinities, a result of regional seasonal rainfall and inflow patterns.

Four field experiments were conducted in the GB and MB systems, each lasting seven days. Previous experiments using similar design demonstrated that an experimental duration of seven days is relevant for studying plankton dynamics in eutrophic waters (Lundgren et al.,

2015; Nielsen et al., 2012). Two experiments were conducted during the late fall and two during late winter. The fall experiments were initiated on November 25 and December 10, 2014 in the GB and MB systems, respectively, and the winter experiments were initiated on February 26 and March 13, 2015 in the GB and MB systems, respectively. These times of the year were chosen to overlap with the historical pre-bloom and bloom periods of *Prymnesium parvum* in inland water bodies of Texas (Roelke et al., 2011). These experiments followed several years of sustained droughts in Texas that started with the 2011 La Niña weather event. By mid-2014, a majority of the state was still in drought with statewide reservoir capacity reduced by one-third. Petroleum pollution from the 2010 Deepwater Horizon platform explosion and an eight-month sustained *Karenia brevis* bloom affected bays over most of Texas' coastline.

Field Methods

Locations in the bay systems where waters were collected for the experiments were influenced by salinity, and collection locations were selected to best match the salinity of the *P. parvum* cultures to be used in the experiments. For both experiments in the GB system, water was collected ~100m away from the shoreline near Kemah, Texas, in upper Galveston Bay. In the MB system in the fall experiment, water was collected near the shore at high tide in western Chocolate Bay. In the winter experiment, water was collected in lower Lavaca Bay near the International Ship Channel. For all experiments, water was collected from a depth of approximately 0.5 m. For the late fall experiments, salinity at the time of collection for GB and MB systems was 19 ppt. For both late winter experiments the salinity was 20 ppt. Temperature, however, varied seasonally and between bay systems. Temperatures were 15°C for GB system and 19°C for MB system during the fall experiments. For winter experiments, temperature for GB system was 10°C and for MB system it was 16°C.

ExperimentalTreatments

All experiments followed a full-factorial (2x2x3) design that included two levels of grazing, two growth phases of *P. parvum*, and three pH levels. Thus, each experiment had 12 treatments that were each deployed in triplicate for a total of 36 experimental units per experiment. Experimental units were comprised of 25 L polycarbonate carboys and 2 L

Figure 4.2. Unfiltered treatments in the Galveston small boat basin.

polycarbonate bottles. The carboys were used for the unfiltered treatments and the bottles used for filtered treatments. Water for treatments using filtered water was filtered immediately upon collection and consolidated into a large container where it was mixed periodically with a large glass stirrer before being added to the 2 L bottles. For the larger size fraction, carboys were filled close to capacity (23L) while onboard the research vessel. All experimental units had headspace enough to ensure buoyancy just below the water's surface, and were tethered to piers. In addition, experimental units (Figure 4.2) were shaded by optically neutral density screening to reduce surface light to irradiance levels similar to the collection depth of 0.5 m (Roelke et al., 2011).

Experimental units containing unfiltered and filtered (63μm) bay water were inoculated

with either stationary- or log-growth phase *Prymnesium parvum* culture. The unfiltered and filtered waters were further manipulated into three pH levels, one ambient and two manipulated through acid additions. Treatments with filtered waters, i.e., having only particles smaller than 63µm, were employed to investigate phytoplankton responses to treatments in the absence of grazing by larger bodied zooplankton, and the unfiltered bay water treatments were used to investigate plankton community responses.

For the GB system, *in-situ* experiments were deployed at the small boat basin of Texas A&M University at Galveston, an area that receives sufficient turbulence through wave action to keep experimental units well-mixed. For the MB system, *in-situ* experiments were deployed at the Texas Parks and Wildlife Department Coastal Fisheries facility in Port O'Connor, again in an area that receives sufficient turbulence to keep experimental units well-mixed.

Plankton Size Fraction

Water designated for the smaller plankton fraction, here referred to as filtered water, was filtered into a large container using a Dolphin^{TM} bucket with a 63µm mesh nylon net (Wildco, Yulee, FL, USA) to exclude larger plankton. The second size fraction, here referred to as unfiltered water, was obtained by passing water through a 153µm cod end. The >153µm portions were subsequently pooled together, gently mixed, and divided into equal aliquots for distribution into the 18 carboys to ensure the same or very similar plankton initial conditions at deployment. This method was employed to minimize the effect of heterogeneity from repeated sampling that can disproportionately affect larger plankton that are present at naturally low population densities.

Prymnesium parvum growth phase

To test the effect of *P. parvum* at different levels of toxicity, experimental units were

inoculated with either log- or stationary-growth *P. parvum.* Research has shown that *P. parvum* in stationary growth phase exerts stronger toxicity on target organisms than log growth culture, so culture from both growth phases was used to represent high and low toxicity conditions, respectively (Lundgren et al., 2015; Shilo, 1967; Granéli and Salomon, 2010). Inoculations were at 10% bloom density of *P. parvum* (=$1x10^6$ cells/L) to better represent conditions shortly after *P. parvum* immigration into a native assemblage.

Prymnesium parvum was grown in the lab in batch cultures at F/2 media concentration in autoclaved RO water adjusted to 20ppt using artificial salt (Instant Ocean). The cultures were incubated in 6 L Erlenmeyer flasks at 20°C for the fall experiments and 14°C for the winter experiments on a 12:12 h light:dark cycle with an irradiance of 200 μmol photons m^{-2} s^{-1} from cool white fluorescent tubes. Cultures were aerated to ensure mixing, and growth was monitored every other day measuring in vivo fluorescence with a Turner Designs 10-AU fluorometer. Cultures designated for log growth phase treatments were kept in log growth phase by replacing 30% of the culture volume every second day with fresh F/2 medium. Cultures designated for the stationary growth phase treatments grew without media replacement until stationary growth phase was reached, which occurred 3–4 weeks after the last media addition.

Manipulation of pH

To manipulate pH in experimental units, HCl was slowly added until the target pH was achieved. For larger-scale marine experiments, acid or base additions are recommended instead of CO_2 bubbling to change pH (Hurd et al., 2009). Moreover, CO_2 bubbling is not recommended if the assemblage has fragile organisms such as some dinoflagellate and ciliate species (Nielsen et al., 2012). The ambient waters in the bay for each experiment were higher than the historical average for each bay. In the fall experiments, Upper Galveston Bay had a pH of 8.2 and

Chocolate Bay in West Matagorda Bay had a pH of 8.7. In the winter experiment, the situation was flipped, and Upper Galveston Bay had the higher ambient pH of 8.7, and in West Matagorda Bay, Lavaca Bay had a pH of 8.3.

For the initiation of experiments, adjustments to pH were made at the deployment site. For treatments using filtered waters, the combined filtered waters (~40 L) were gently mixed for several minutes, and then dispersed in two liter aliquots into six of the experimental bottles. The remaining filtered water (~28 L) was then manipulated to lower pH levels for those treatments. To do this, HCl was dispersed gradually into a large plastic container, gently stirred until the target pH of 7.5 was reached, and two liter at a time removed until 6 bottles were filled. To the remaining water, HCl was again dispersed gradually and gently stirred until the target pH of 7.0 was reached, and two liters of water at a time were extracted until 6 bottles were filled. A handheld pH meter (EcoTestr pH2) was used to monitor pH level as acid additions were made. The pH of the carboys for the amended pH treatments was manipulated individually. Approximately 5ml HCl was initially added to carboys designated for the 7.5 pH treatments, and 10ml HCl was added to the carboys designated for the 7.0 pH treatments. The carboys were tipped over on their sides 10 times to gently mix the contents. After several minutes, a pH reading was made and acid additions made as necessary. This process continued until 6 carboys were at 7.5 pH and 6 carboys were at 7.0 pH.

Response variables

Response variables included enumeration of *P. parvum;* chl-*a* concentrations to characterize total phytoplankton biomass; *P. parvum* and zooplankton biovolumes; toxicity using bioassays of juvenile silversides (*Menidia beryllina*); and concentrations of inorganic nutrients and urea. Initial phytoplankton and zooplankton densities were determined from water collected

at the site on the day of initiation. Zooplankton enumeration and biovolume, toxicity bioassays and inorganic nutrients were assessed at the beginning and end of the experiment; mid-point samplings were done to capture short-term plankton responses. All other response variables were recorded at 4 time points: day 0 (experiment initiation), day 2, day 4, and day 7 (experiment termination). Mid-point samplings were made to capture short-term plankton responses, and each container was checked for pH levels and adjusted to the target pH if necessary. In the first experiment, the second midpoint sampling and pH adjustments occurred on day 5.

Phytoplankton samples were collected from the well-mixed experimental units in 100 ml aliquots from carboys, and 25-100ml aliquots from bottles. The lesser volume was chosen for the bottles to minimize the total volume extracted from bottles over the course of the experiment. The samples were preserved using 25% glutaraldehyde (5%, v/v). The Utermohl (1958) settling technique was used to determine population densities of all phytoplankton. A one milliliter sub-sample was settled for 24 hours and counted using an inverted light microscope (400x, Leica Microsystems). An initial target goal to count 150–200 cells per sample was amended due to low *P. parvum* densities across treatments for all experiments. Instead, all *P. parvum* cells were counted on 20 randomly selected fields of view. Biovolume of each *P. parvum* cell was determined using the equation for ellipsoid body shape (Hillebrand et al., 1999).

Initial zooplankton samples from the water collection site were collected using a Schindler trap (20µm mesh size), concentrating a 12 L sample to 50 ml. At the termination of each experiment, zooplankton samples were collected by passing 17 L of experimental water through a 63 µm screened Dolphin bucket. For preservation of zooplankton samples, 2% buffered formalin (10%, v/v) was used. Subsamples of 5–10ml were settled for 24 hours and then counted with an inverted light microscope (40x and 200x, Leica Microsystems). Biovolume

of each counted zooplankter was determined by measuring dimensions according to geometric shapes similar to body shapes (Wetzel and Likens, 1991). Zooplankton were grouped as adult copepods, copepod nauplii, tintinnids and total protozoa.

For determination of chl-*a* concentrations, duplicate samples of 50ml from each experimental unit were filtered through GF/F filters according to standard fluorometric procedures (APHA, 2006). Pigments were extracted overnight in 90% acetone, centrifuged and analyzed in a Turner designs 10-AU fluorometer, using the acidification method. Nutrient concentrations were analyzed with autoanalyzer methodology and included ammonium, urea, silica, orthophosphate and the sum of nitrate and nitrite (Armstrong and Sterns, 1967; Harwood and Kuhn, 1970). The initial aliquot passing through the filtration apparatus of filtrate for nutrient analysis was discarded to negate possible dilution effects from residual rinse water. The GF/F filters used for filtrate destined for nutrient analysis were washed with 10% HCl and rinsed in a process repeated three times, and the filters dried prior to use. This was done to remove any nitrate and phosphate present on the filter due to the manufacturing process.

Initial ambient toxicity was determined from samples of unfiltered bay water inoculated with stationary- and log-growth phase *Prymnesium parvum* at $1x10^6$ cells L^{-1} density. Toxicity was also measured from each experimental unit at the termination of each experiment. For this purpose, standardized 24-h static toxicity assays with the juvenile silverside minnows (*Menidia beryllina*), a common fish model for assessing ambient toxicity in marine and estuarine systems, were used. Samples were collected and stored cold and in the dark while transported to the laboratory where the fish bioassays were initiated within 24 h. Toxicity assays followed standardized methods using a 0.5 dilution series with artificial sea water prepared to match the salinity of each bay (US EPA, 2002).

Data Analysis

Two and three-way ANOVAS were performed on proportional changes of P. parvum densities, chl-*a* and phaeophytin concentration at the termination of the experiments. All statistical analyses were performed in Matlab (The MathWorks, Inc.) with results noted as significant when $p < 0.05$.

Results

Overall, there were few significant differences between treatments of *P. parvum* growth phase, pH level or size fraction. Details are listed in each subsection below.

I was not able to make seasonal comparisons for the filtered treatments because some of the manipulated pH treatments resulted in pH levels lower than the target, so those units were discarded from all analyses. The unfiltered treatments for all experiments met the target level of manipulation, so they are included in the results for seasonal differences.

There was no acute toxicity in these experiments and thus LC50 values could not be calculated.

For each experiment initiation, I successfully manipulated the pH to the experimental target levels. However, starting with the first midpoint, there was variability in the level of pH for many experimental units each time they were measured (Appendix 1 following this chapter has all timepoint pH levels for each experiment). This greatly affected the precision in manipulating the pH back down to the target level (either 7.5 or 7.0), especially the filtered fraction size fraction treatments, which were deployed in 2 liter bottles. I "overshot" or added too much HCl for several of these bottles throughout the experiments, and these replicates have been removed from all analyses.

Prymnesium parvum density

Proportional changes in *P. parvum* cell density from the initial condition to the final condition were analyzed with a three-way ANOVA for differences between growth phase, pH and size fraction. Results show that altogether, there were very few statistically significant differences in *P. parvum* density in each of the four experiments, with no significant three-way interactions. There were also no significant differences between or within any treatment for either Galveston Bay experiment. However, there was a significant difference between the filtered and unfiltered treatments for both Matagorda Bay experiments ($p < 0.05$). In the Matagorda Bay winter experiment, there was a significant difference in pH ($p = 0.01$).

Figure 4.3 shows the changes in *P. parvum* density at the initiation and termination of each experiment. Generally, the graphs show that *P. parvum* density decreases after experiment initiation, and in the filtered fraction, many units show an increase in density, though the densities never increase over the inoculation density. In the zooplankton treatment, different results seem to occur in that the *P. parvum* densities do not respond with as robust an increase over time as the smaller size fraction treatments, and many units maintain a very low *P. parvum* population.

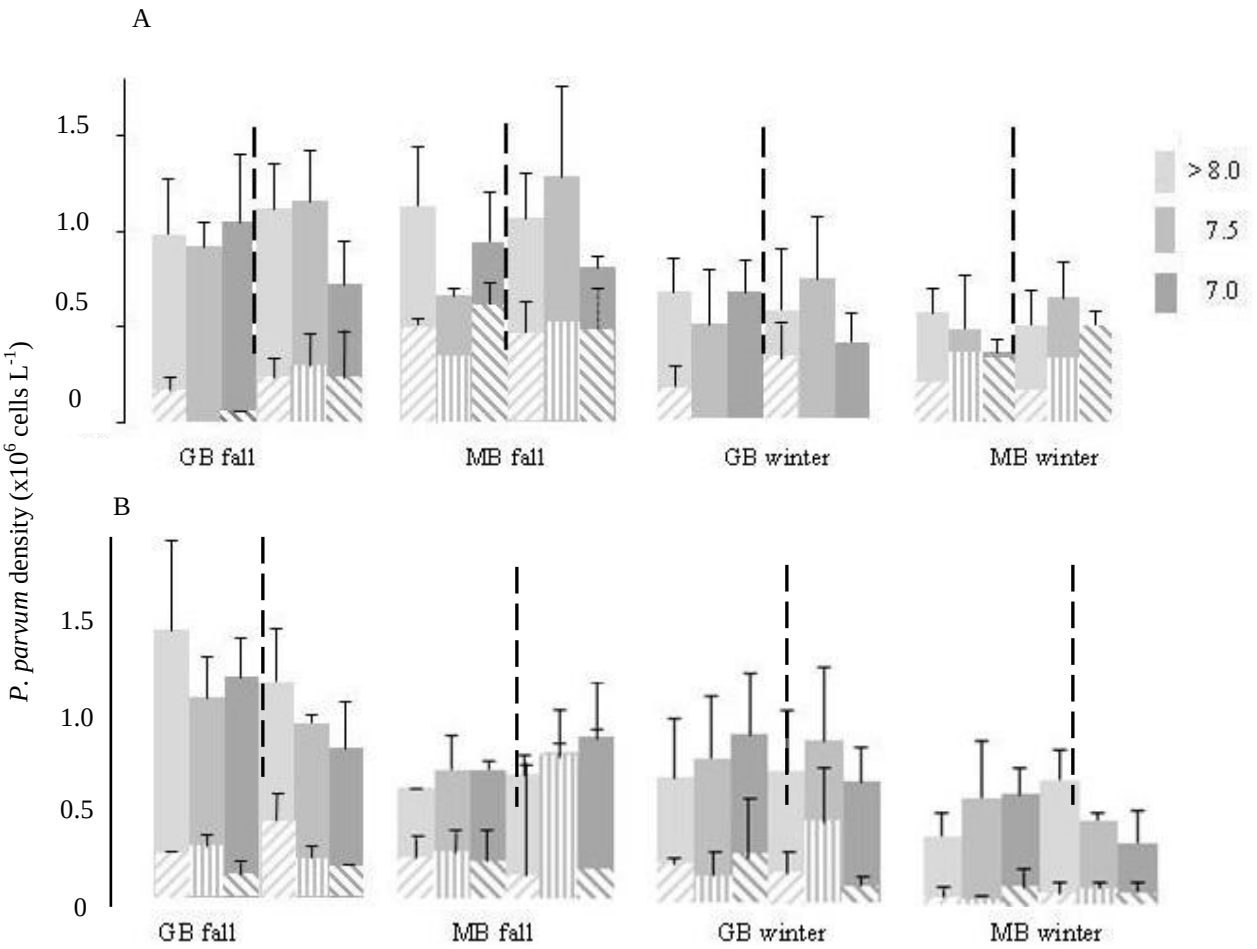

Figure 4.3. Average *P. parvum* densities at t-initial (solid bars) and t-final (striped bars) for filtered (panel A) and unfiltered (panel B) treatments each experiment. For all experiments and all treatments, *P. parvum* densities never increased above the inoculation density. Bars to the left of the vertical dotted line are stationary treatments; bars to the right of the dotted line are log treatments. Absence of striped bars indicates no data at t-final for those treatments. Dotted error bars refer to t-final treatments.

Chl-a concentration

Chl-*a* results were different between the two bays and do not seem to suggest any seasonal trends. The Galveston Bay fall and the Matagorda Bay winter experiments had increases in chl-*a* for all treatments by the end of those experiments, whereas chl-*a* decreased for all treatments in the Matagorda Bay fall and Galveston Bay winter experiments (Table 4.1). The concentrations at the end of the experiment for the Galveston Bay fall were five times higher than for the other experiments (> 30 μg/L). The concentrations for the other three experiments

were comparable to each other at the end of those experiments and ranged from 4 μg /L to 10 μg /L. The Matagorda Bay fall experiment was distinct in its unfiltered treatments, which were consistently lower than the filtered fraction treatments at the end of that experiment, whereas for the other three experiments, chl-*a* concentrations for all units were within similar

Table 4.1 Mean chl-*a* and standard deviation (SD) at experiment initiation (t0) and termination (tf) for all experiments Experimental treatments that did not meet the target pH manipulation level at any point have been removed. N=3 for all treatments unless otherwise noted

GB fall (filtered)	**t0 mean (+SD)**	**tf mean (+SD)**	**GB fall (unfiltered)**	**t0 mean (+SD)**	**tf mean (+SD)**
> 8.0	9.34 (0.78)	76.78 (19.87)	> 8.0	11.63 (1.04)	44.27 (11.14)
7.5	14.89 (2.03)	--	7.5	12.84 (0.09)	32.44 (20.62)
7.0 n=1	15.19	35.39	7.0 n=2	13.75 (2.03)	40.56 (7.86)
> 8.0	9.21 (0.42)	20.86 (13)	> 8.0	13.57 (1.18)	44.17 (9.72)
7.5 n=2	13.26 (1.43)	29.07 (18.71)	7.5	10.16 (6.85)	39.94 (15.65)
7.0 n=2	14.38 (0.32)	36.29 (13.91)	7.0	10.29 (4.38)	33.02 (18.2)
MB fall (filtered)	**t0 mean (+SD)**	**tf mean (+SD)**	**MB fall (unfiltered)**	**t0 mean (+SD)**	**tf mean (+SD)**
> 8.0	10.14 (0.22)	5.21 (1.54)	> 8.0	10.76 (2.96)	2.45 (0.36)
7.5 n=1	10.25	5.51	7.5 n=2	8.14 (0.11)	1.92 (0.57)
7.0 n=1	12.6	6.87	7.0	6.98 (1.09)	2.87 (0.69)
> 8.0	9.03 (1.78)	4.16 (1.37)	> 8.0	8.45 (0.66)	3.4 (0.89)
7.5 n=2	9.69 (1.17)	9.17 (3.2)	7.5	8.63 (1.58)	2.62 (0.7)
7.0	8.27 (1.11)	8.74 (3.26)	7.0	9.04 (1.41)	2.71 (0.14)
GB winter (filtered)	**t0 mean (+SD)**	**tf mean (+SD)**	**GB winter (unfiltered)**	**t0 mean (+SD)**	**tf mean (+SD)**
> 8.0	16.4 (2.0)	3.85 (1.69)	> 8.0	16.06 (1.19)	5.39 (2.33)
removed	--	--	7.5	15.31 (1.45)	4.75 (0.42)
removed	--	--	7.0	13.54 (3.89)	4.37 (1.08)
> 8.0	15.63 (1.29)	4.58 (0.79)	> 8.0	15.24 (0.87)	5.64 (0.86)
removed	--	--	7.5	12.85 (2.67)	4.34 (1.01)
removed	--	--	7.0	15.59 (2.13)	5.25 (1.36)
MB winter (filtered)	**t0 mean (+SD)**	**tf mean (+SD)**	**MB winter (unfiltered)**	**t0 mean (+SD)**	**tf mean (+SD)**
> 8.0	3.33 (0.29)	5.17 (0.31)	> 8.0	2.67 (0.13)	3.91 (1.58)
7.5	3.38 (0.31)	5.48 (0.53)	7.5	2.29 (0.01)	5.9 (0.25)
7.0 n=2	3.35 (0.44)	4.74 (1.52)	7.0 n=2	2.24 (0)	6.37 (0.8)
> 8.0	3.26 (0.21)	3.46 (0.92)	> 8.0	2.42 (0.22)	4.98 (0.55)
7.5 n=2	3.18 (0.31)	5.04 (0.85)	7.5	2.67 (0.09)	3.65 (0.66)
7.0	3.63 (0.44)	9.75 (4.67)	7.0	2.68 (0.43)	5.54 (1.02)

ranges at the conclusion of those experiments.

As with analysis of *P. parvum* density, results of a three-way ANOVA for differences between growth phase, pH and size fraction using proportional changes in chl-*a* concentration from experiment start to completion show that there were no significant three-way interactions for any of the experiments. However, the same factors that were significant in *P. parvum* density were found to be significant here. There was a significant difference between the filtered and unfiltered fraction treatments for both Matagorda Bay experiments ($p < 0.05$). As with *P. parvum* density, in the Matagorda Bay winter experiment there was a significant difference in chl-*a* with pH level ($p = 0.01$). Notably, in the Matagorda Bay winter experiment, there was also a significant interaction between *P. parvum* growth phase and size fraction ($p = 0.03$), a significance not found for this experiment in the *P. parvum* density response.

As with the *P. parvum* density response, there were also no significant differences between or within any treatment for either Galveston Bay experiment.

Phaeophytin concentration

Results here are mostly consistent with what has been described above; there are no significant three way interactions for any experiment, nor were there significant differences between or within any treatment for either Galveston Bay experiment. For the Matagorda Bay fall experiment, a three-way ANOVA shows a significant difference of size fraction for phaeophytin concentration ($p < 0.05$); a followup two-way ANOVA analyzing both fractions separately, however, does not indicate which size fraction has within-treatment significance. However, unlike the results for *P. parvum* density and chl-*a* concentration, there was no significant difference in size fraction or pH for the Matagorda Bay winter experiment.

Zooplankton biovolume

Zooplankton biovolume for each experiment was measured for taxa in the unfiltered

treatments (Figure 4.4). The total zooplankton biovolume was highest for the Matagorda winter experiment (1.87 x10^{11} μm^3/L), lowest for Matagorda Bay during the fall experiment (4.17 x10^{10} μm^3/L). The values for the Galveston Bay fall and winter experiments were 1.72 x$10^{11}$$\mu m^3$/L and 1.09 x$10^{11}$ μm^3/L, respectively. There were differences between growth stage within each experiment. For all except the Matagorda Bay winter experiment, total biovolume was highest in stationary treatments. Three main taxonomic groups were identified for each experiment: adult copepods, nauplii, and protozoa. Very few rotifers (*Keratella* spp) were observed during microscopy, though protozoan tintinnids, oligotrichs and vorticella were numerous. Loricate tintinnids were especially abundant in the fall Matagorda Bay experiment. Harpacticoid copepods were more numerous than calenoid copepods, and copepod taxa dominated the biovolume for all experiments. The Galveston bay winter experiment had the highest species richness (10 species), though richness was similar among all four experiments.

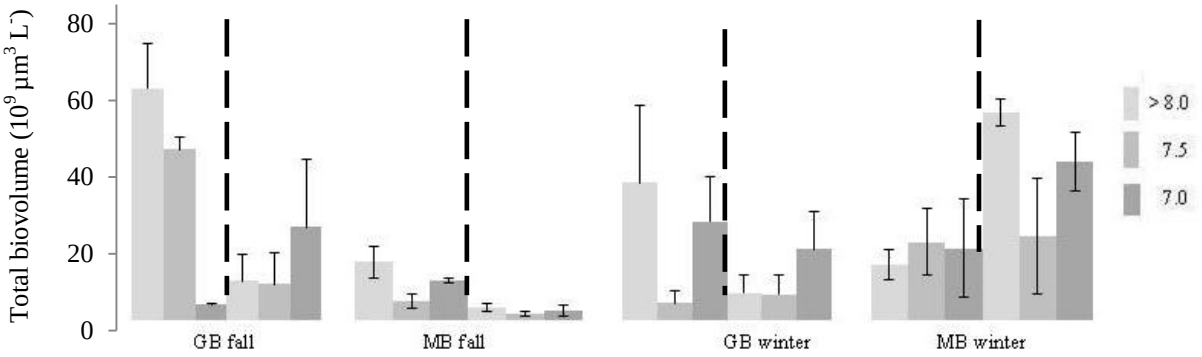

Figure 4.4 Average zooplankton biovolume at t-final for each experiment. Bars to the left of the vertical dotted line are stationary treatments; bars to the right of the dotted line are log treatments.

Inorganic nutrient levels

The initial nutrient level ratios and concentrations (ambient) were different for each experiment. On the whole, Galveston Bay had higher average inorganic nutrient concentrations than Matagorda Bay. Nitrate averaged 26.78 μM in the Galveston fall experiment, and phosphate averaged 5.28 μM, whereas in the Matagorda fall experiment, nitrate averaged 0.33 μM and phosphate averaged 0.94 μM. In the winter experiments, nitrate was lower in Galveston compared to Matagorda, with a concentration of 1.40 μM, whereas Matagorda started with 12.27 μM. Initial phosphate concentration in the Galveston winter experiment was 2.04 μM and Matagorda was 0.84 μM. Nitrite, ammonium and urea were higher in Galveston for the start of both experiments, and silicate was very high for all experiments.

Generally, at the conclusion of each experiment the nutrient levels in the unfiltered treatments were not depleted, except for the ambient stationary and low log treatments, in which nutrients were close to depleted. Silicate was never limiting for any of the twelve unfiltered treatments and increased by the end of most experiments. In the filtered treatments, nitrate was depleted for all phytoplankton treatments, though some phosphate remained in containers of two fall experiments.

In the Galveston Bay fall experiment, there was excess nitrate in all containers with zooplankton except ambient pH treatments that had stationary *P. parvum* added. There was also excess nitrate in the Matagorda Bay winter experiment for all treatments except the medium pH stationary and low log treatments.

Summary plots of changes in *P. parvum* density (Figure 4.5) and phaeophytin concentration (Figure 4.6) over the course of the experiment were also created and separated by size fraction. Figure 4.5 shows the relationship between proportional changes in *P. parvum*

density at experiment initiation to the population minima (the lowest observed density), and from the population minima to the final density for each experimental unit. The graph with filtered fraction containers (panel A) shows that many of the units recovered from their lowest observed density (population minima) of *P. parvum* and began to increase in density by the end of the experiment. The graph with unfiltered treatments (panel B) shows that the majority of these units either did not increase beyond the observed density minima, or increased less than than the filtered units did. This effect is strongest with the Matagorda Bay winter experiment (green open circles), supported by the statistics reported above. It should be noted here that there are fewer units represented in panel A because some filtered treatments were discarded from analysis due to missing the target pH manipulation.

Figure 4.6 shows changes in phaeophytin concentration over the course of the experiment with panels separated by size fraction. Here there is a different trend than is seen in Figure 4.5. These graphs suggest an overall trend of higher phaeophytin concentration in the filtered treatment containers by experiments' termination compared to the unfiltered treatment containers.

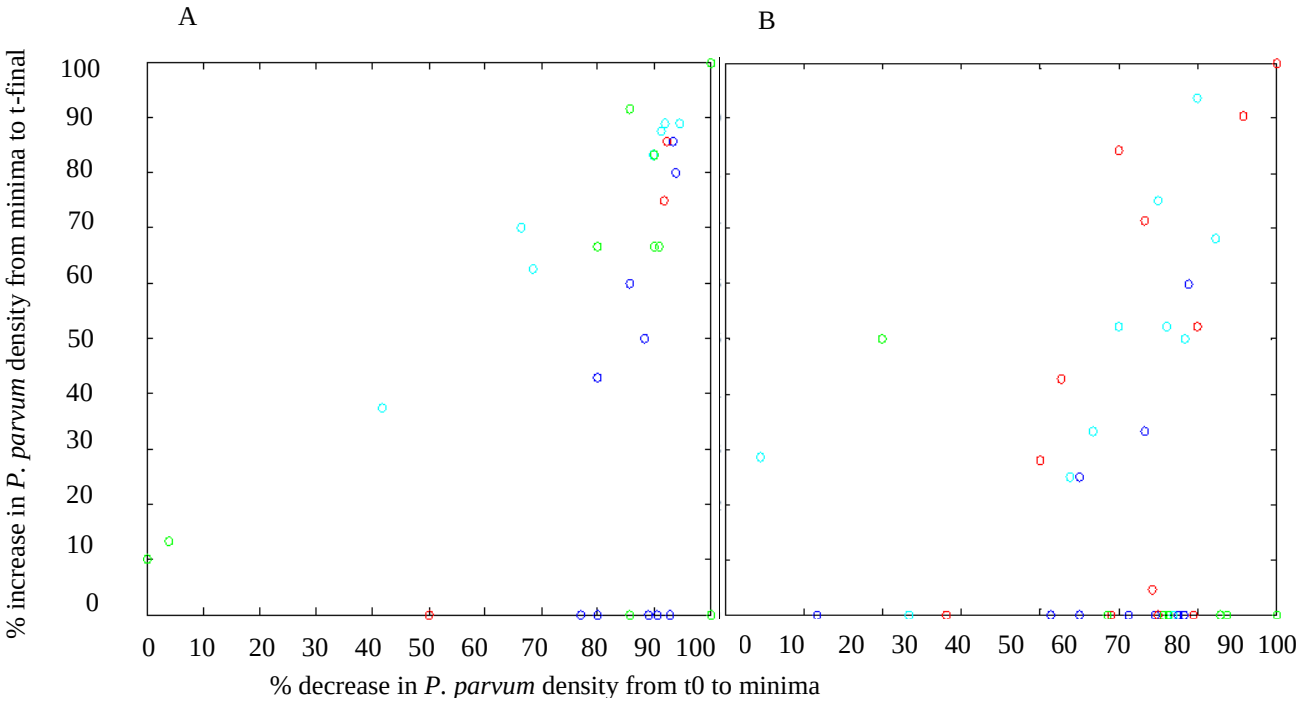

Figure 4.5 Relationship between proportional decreases in *P. parvum* density at experiment initiation to the population minima (x-axis) and *P. parvum* density increases from the population minima to the end of the experiment (y-axis) for filtered treatments (panel A) and unfiltered treatments (panel B). Each open circle represents one replicate and is identified according to the following colors: blue-Galveston Bay fall; cyan-Matagorda bay fall; red-Galveston Bay winter; green-Matagorda Bay winter. Convergence of markers in the upper left corner of panel A indicates a greater increase in *P. parvum* density compared to unfiltered replicates in panel B.

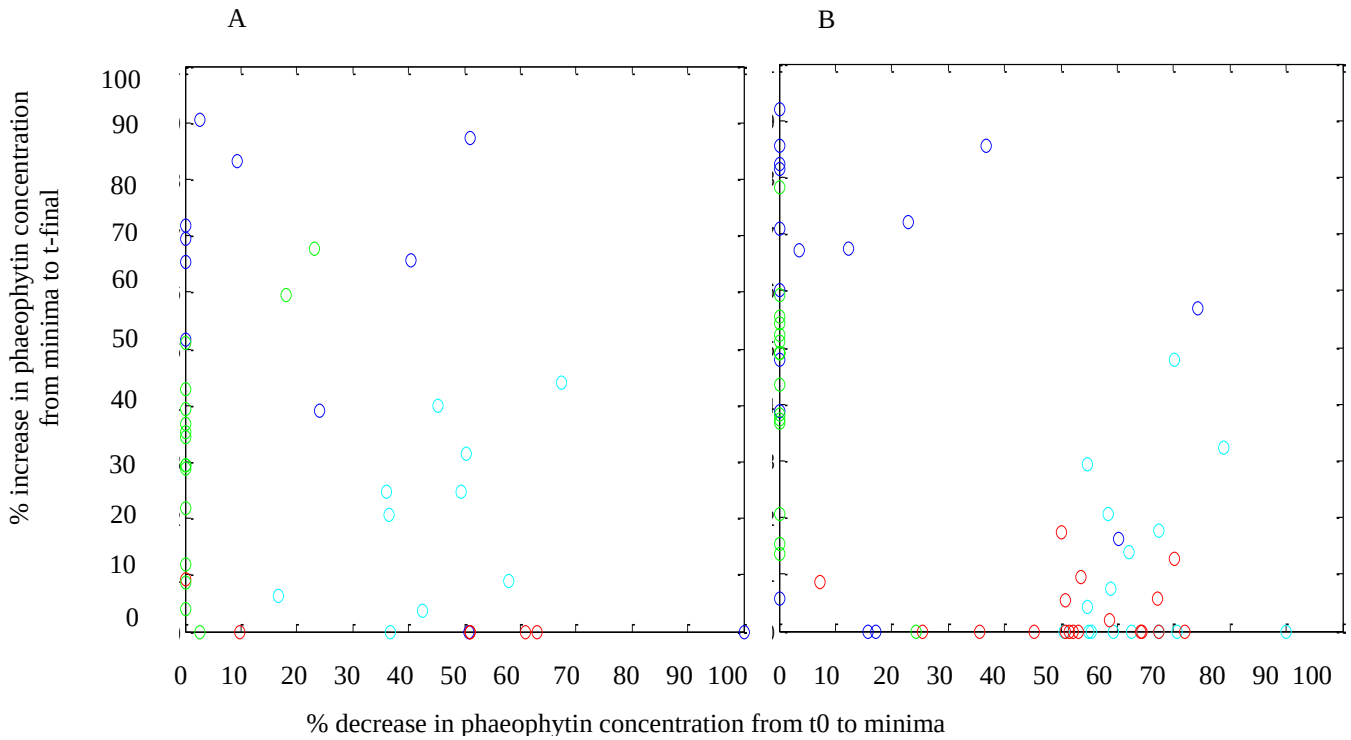

Figure 4.6 Relationship between proportional decreases in phaeophytin concentration at experiment initiation to the concentration minima (x-axis) and increases from the concentration minima to the end of the experiment (y-axis) for filtered treatments (panel A) and unfiltered treatments (panel B). The marker colors are the same as in figure 4.5.

Discussion

In these experiments, there is an emergent trend showing a difference in *Prymnesium parvum* response to pH levels between the size fractions. Many filtered treatments experienced increases in *P. parvum* densities from a minimum point by the end of the experiment, contrasted with treatments with zooplankton, which are characterized less or no rebound in *P. parvum* density by the end of the experiment. This can be explained by differences in grazing effects between the two treatment types. Though there was no demonstrated toxicity of *P. parvum* in these experiments that might enable it to form a bloom, the results suggest that *P. parvum* can increase in abundance in the absence of large grazers (Figure 4.5A). Thus, grazing pressure by large zooplankton in the bay may keep *P. parvum* density low if the *P. parvum* densities are low or moderate.

On the other hand, smaller grazers, whose presence in the filtered treatments is certain given the high phaeophytin concentrations and my observations of ciliates, may not be able to control even low densities of *P. parvum*. I noted several HAB species during microscopy counts. *Dinophysis* spp., *Pseudonitzschia* spp. and *Prorocentrum* spp. were not uncommon, though none reached the abundance of *P. parvum* for any treatment at any time point. With these observations it is reasonable to assume that other HAB species did not exert a significant effect on *P. parvum* growth. However, the differences in phaeophytin concentration between the filtered and unfiltered treatments may explain some of the observed effects. In marine and freshwater systems, grazing of phytoplankton degrades chlorophyll into phaeopigments (Fundel et al., 1998). The size of the herbivore is relevant, however, in the amount of phaeophytin that is created, demonstrated by mesocosm experiments of smaller grazers that resulted in a higher concentration of phaeopigments when compared to large zooplankton species (Carpenter and

Bergquist, 1985). In the filtered units (Figure 4.6), phaeophytin concentration increases by the end of the experiment, suggesting grazing of phytoplankton over the course of the experiment. Presence of smaller grazers is expected in the filtered units, and I observed small oligotrich ciliates *(Strombidium* spp., *Myrionecta* spp.), which are distinct from oligotrich group identified in the zooplankton containers. The unfiltered treatments show a pronounced decrease in phaeophytin concentration, with many units maintaining low concentrations by the end of the experiment, also consistent with previous experiments in which there is less phaeophytin present with large grazers such as copepods (Carpenter and Bergquist, 1985). Some cyanobacteria have relatively more chl-*b* (Paerl 2003), so one interpretation of high phaeophytin values in the filtered treatments could be high cyanobacteria densities. However, although I did not quantify other phytoplankton species, cyanobacterial populations were not high for any experiment. The phaeophytin graphs are provided to support the idea that despite grazing activity in the filtered containers, *P. parvum* was able to increase in abundance more than in the unfiltered treatments which had a higher density of large zooplankton.

The average final chl-*a* concentrations for the Galveston Bay fall treatments were relatively high compared to the other experiments. This may be explained in part by the high ambient nutrient levels on the first day of the experiment. However, the results for the chl-*a* are not straightforward in light of the zooplankton biovolume data. In most experiments, total zooplankton biovolume was highest in stationary treatments, which is consistent with the results in Lundgren et al. (2015).

The initial pH in both bays was similar to each other, with a range of 8.2-8.7. This range is well within the known range for maintaining *P. parvum* allelotoxicity. Experimental studies and modelling suggest that *P. parvum* exhibits its highest toxicity at higher and lower salinity

ranges (Baker et al., 2007). Conditions during the bay experiments, however, were close to ranges considered optimal for growth of *P. parvum* and were not within the ranges for salinity and temperature for high toxicity (Baker et al., 2007), so the lack of toxicity effects from *P. parvum* in these experiments is not surprising.

P. parvum abundance showed little significant difference between pH levels, though that does not negate the possibility that it was exerting an interference effect on plankton in these treatments. However, the factor that influenced *P. parvum* growth in the filtered treatments is not significant enough to overcome the effects of zooplankton grazing. It has been demonstrated previously that at higher densities, *P. parvum* can form toxic blooms in Galveston Bay waters (Lundgren et al. 2015). Thus, it is reasonable to expect the same dynamics would occur in Matagorda Bay waters.

The alkalinity of these bays is decreasing over the last 40 years (Hu et al. 2015). Further, the alkalinity of East Matagorda Bay is decreasing at the fastest rate of any bay in Texas, and is decreasing at a rate approximately four times faster than Galveston Bay (Hu et al. 2015). Scenarios of estuarine acidification in Texas bays may serve to dampen long-term potential of *P. parvum* blooms. However, given the ability of *P. parvum* to increase its toxicity with an increase in pH over short time scales, blooms of other autotrophs may raise pH sufficiently in a localized area, favoring an increase in *P. parvum* toxicity.

Additionally, the near-depletion of inorganic nutrients in most filtered fraction treatments allows for the possibility that *P. parvum* allelotoxicity may have increased over the duration of the experiment. Increased or induced toxicity in phytoplankton in response to limiting or imbalanced ambient nutrient levels occurs for some phytoplankton species, including *P. parvum* (Plumley 1997; Sunda, 2006; Hardison et al., 2012; Errera et al., 2008; Graneli et al., 2012). Loss

of toxicity at lower pH is variable, however (Ulitzer and Shilo, 1970; Shilo and Aschner, 1953; Southard and Klein, 2005), with a complete loss of toxicity only below pH 6.5 (McLaughlin 1958).

My efforts to maintain a lower pH between manipulations may have been impeded by the alkalinity of coastal waters, which provides a buffer against abrupt changes in pH, and some experimental units required more HCl than others. The 2L bottles, which contained the filtered treatments, had a greater range of variability in pH levels between manipulations, whereas pH was much more stable between manipulations in the 23L carboys, which contained the unfiltered treatments. This stability may be due in part to the effects of herbivory impacting potential increases in pH due to photosynthesis in the larger carboys.

Conclusions

At ecologically relevant densities, a combination of factors may need to exist to promote a bloom of *P. parvum* in Texas bay systems. These experiments do not support the idea that pH alone exerts a strong influence on the toxicity of *P. parvum* . However, differences in the response of *P. parvum* in the presence of large grazers suggest that without such biologic controls, this species can readily increase its abundance.

References

American Public Health Association, American Water Works Association, Water Environment Foundation, 1998. Standard Methods for the Examination of Water and Wastewater, 20th ed. American Public Health Association, Washington, DC.

Anderson, J.B., Rodriguez, A.B. (Eds.), 2008. Response of Upper Gulf Coast Estuaries to Holocene Climate Change and Sea-Level Rise. Geological Society of America Special Paper 443, 146 pp.

Armstrong, F.A., Sterns, C.R., 1967. The measurement of upwelling and subsequent biological processes by means of the Technicon Autoanalyzer and associated equipment. Deep-Sea Res. I 14, 381–389.

Baker, J.W., J.P. Grover, B.W. Brooks, F. Uren˜a-Boeck, D.L. Roelke, R. Errera, and R.L. Kiesling. 2007. Growth and toxicity of Prymnesium parvum (Haptophyta) as a function of salinity, light, and temperature. Journal of Phycology 43 (2): 219–227.

Carpenter, S.R. and Bergquist, A.M. (1985) Experimental tests of grazing indicators based on chlorophyll a degradation products. Arch. Hydrobioi, 102, 303-317.

Criner, O., and M.D. Johnican 2001. Update 2000: current status and historical trends of the environmental health of Galveston Bay. Galveston Bay Estuary Program. Webster, Texas.

Errera, R.M., Roelke, D.L., Kiesling, R., Brooks, B.W., Grover, J.P., Schwierzke, L., Urena-Boeck, F., Baker, J.W., Pinckney, J.L., 2008. The effect of imbalanced nutrients and immigration on Prymnesium parvum community dominance and toxicity: results from in-lake microcosm experiments, Texas, US. Aquat. Microb. Ecol. 52, 33–44.

Fistarol, G.O., Legrand, C., and Grane´li, E., 2003. Allelopathic effect of Prymnesium parvum on a natural plankton community. Marine Ecology Progress Series 255, 115–125.

Fiori, E., Vidyarathna, N., Hagström, J., Pistocchi, R., Graneli, E. 2012. Influence of Light on Prymnesium parvum Growth, Toxicity and Mixotrophy. Linnaeus Eco-Tech. DOI: https://doi.org/10.15626/Eco-Tech.2012.025

Granéli, E., Johansson, N., 2003. Increase in the production of allelopathic substances by Prymnesium parvum cells grown under N- or P-deficient conditions. Harmful Algae 2:7, 135–145.

Granéli, E., Hansen, P.J., 2006. Allelopathy in harmful algae: a mechanism to compete for resources? In: Granéli, E., Turner, J.T. (Eds.), Ecology of Harmful Algae, Ecological Studies, vol. 189. Springer-Verlag, Berlin, Heidelberg, Germany, pp. 189–201.

Granéli, E., Salomon, P.S., 2010. Factors influencing allelopathy and toxicity in Prymnesium parvum. J. Am. Water Resour. Assoc. 46, 108–120.

Granéli, E., B. Edvardsen, D.L. Roelke, and J. A. Hagstrom. 2012. The ecophysiology and bloom dynamics of *Prymnesium spp.* Harmful Algae. 14: 260-270.

Hillebrand, Durselen, C., Kirschtel, D., Pollingher, U., and Zohary, T. (1999). Biovolume Calculation for Pelagic and Benthic Microalgae. J. Phycol. 35, 403-424.

Hinga, K.R. 1992. Co-occurrence of dinoflagellate blooms and high pH in marine enclosures. Mar. Ecol. Prog. Ser. 86: 181-187.

Hu, X., J.B. Pollack, M.R. McCutcheon, P.A. Montagna, Z. Ouyang. 2015. Long-Term Alkalinity Decrease and Acidification of Estuaries in Northwestern Gulf of Mexico. Environmental Science & Technology. 49: 3401−3409. doi: 10.1021/es505945p

Hurd, Catriona L., Christopher Hepburn, Kim Currie, John Raven, Keith Hunter. 2009. Testing the Effects of Ocean Acidification on Algal Metabolism: Considerations for Experimental Designs, J. Phycol (45):1236-1251

James, T., and A. De La Cruz. 1989. Prymnesium parvum Carter (Chrysophyceae) as a suspect of mass mortalities of fish and shellfish communities in western Texas. Texas Journal of Science 41(4):429-430.

Larsen, A., Eikrem, W. & Paasche, E. 1993. Growth and toxicity in Prymnesium patelliferum (Prymnesiophyceae) isolated from Norwegian waters. Can. J. Bot. 71:1357–62.

Larsen A; Bryant S, 1998. Growth rate and toxicity of Prymnesium parvum and Prymnesium patelliferum (Haptophyta) in response to changes in salinity, light and temperature. Sarsia, 83(5):409-418.

Fundel, Barbara, Hans-Bernd Stich, Hans Schmid and Gerhard Maier. 1998. Can phaeopigments be used as markers for Daphnia grazing in Lake Constance? Journal of Plankton Research Vol.20 no.8 pp.1449-1462.

Hardison D. Sunda, W., Litaker, R., Shea, D., and Tester, P. 2012. Nitrogen Limitation Increases Brevetoxins in Karenia Brevis (Dinophyceae): Implications for Bloom Toxicity.

Harwood, J.E., Kuhn, A.L., 1970. A colorimetric method for ammonia in natural waters. Water Resour. 4, 805–811.

Legrand C, Rengefors K, Fistarol GO, Granéli E. 2003. Allelopathy in phytoplankton—biochemical, ecological, and evolutionary aspects. Phycologia 42:406–419.

Lindholm, Tore, Petra Öhman, Katriina Kurki-Helasmo, Brendan Kincaid & Jussi Meriluoto (1999) Toxic algae and fish mortality in a brackish-water lake in Åland, SW Finland, Hydrobiologia 397: 109–120, 1999.

Liu, Amy E. Koid, Ramon Terrado, Victoria Campbell, David A. Caron, and Karla B. Heidelberg. 2015. Changes in gene expression of Prymnesium parvum induced by nitrogen and phosphorus limitation. Front Microbiol. 2015; 6: 631. doi: 10.3389/fmicb.2015.00631

Lundgren, V.M., D.L. Roelke, B.W. Brooks, E. Graneli, S.L. Davis, T. Baty and W.C. Scott. 2015. Prymnesium parvum invasion success into coastal bays of the Gulf of Mexico: Galveston Bay case study. Harmful Algae. 43: 31–45.

McLaughlin, J. 1958. Euryhaline chrysomonads: nutrition and toxigensis in Prymnesium parvum, with notes on Isochrysis galbana and Monochrysis lutheri. Journal of Protozoology 5(1):75-81.

Nielsen, L. T., G.M. Hallegraeff, S.W. Wright, and P.J. Hansen. 2012. Effects of experimental seawater acidification on an estuarine plankton community Aquat. Microb. Ecol. 65: 271–285.

Plumley, F. G. 1997. Marine algal toxins: biochemistry, genetics, and molecular biology. Limnol. Oceanogr. 42:1252–64.

Prosser, K.N., T.W. Valenti, Jr., N.J. Hayden, M.T. Neisch, N.C. Hewitt, G.D. Umphres, G.M. Gable, J.P. Grover, D.L. Roelke, B.W. Brooks. 2012. Low pH preempts bloom development of a toxic haptophyte. Harmful Algae. 20:156–164.

Roelke, Daniel L., Reagan M. Errera, Richard Kiesling, Bryan W. Brooks, James P. Grover, Leslie Schwierzke, Fabiola Ureña-Boeck, Jason Baker, James L. Pinckney. 2007.

Effects of nutrient enrichment on Prymnesium parvum population dynamics and toxicity: results from field experiments, Lake Possum Kingdom, USA. Aquat Microb Ecol Vol. 46: 125–140.

Roelke, D.L., Grover, J.P., Brooks, B.W., Glass, J., Buzan, D., Southard, G.M., Fries, L., Gable, G.M., Schwierzke-Wade, L., Byrd, M., Nelson, J., 2011. A decade of fish-killing Prymnesium parvum blooms in Texas: roles of inflow and salinity. J. Plankton Res. 33, 243–253.

Sager, D.R., A. Barkoh, D.L. Buzan, L.T. Fries, J.A. Glass, G.L. Kurten, J.J. Ralph, E.J. Singhurst, G.M. Southard, and E. Swanson. 2008. Toxic Prymnesium parvum: A potential threat to U.S. reservoirs. In M.S. Allen, S. Sammons, and M.J. Macina (Eds.), Balancing fisheries management and water uses for impounded river systems (pp. 261-273), American Fisheries Society, Symposium 62, Bethesda, MD.

Schwierzke, L., Roelke, D. Brooks, B., Grover, J.P., Valenti, T., Lahousse, M., Miller, C. and Pinckney, J. 2010. Journal of American Water Resources Association, 46:1, 63-75.

Shilo, M., and M. Aschner. 1953. Factors governing the toxicity of cultures containing the phytoflagellate *Prymnesium parvum* carter. Journal of General Microbiology. 8(3): 333–343.

Shilo, M. 1967. Formation and Mode of Action of Algal Toxins. Bacteriological Reviews. Vol. 31, No. 3, p. 180-193.

Southard, Greg M. and David Klein. September 2005. Effects of pH on Prymnesium parvum Cell Viability and Toxicity. Management of Prymnesium parvum at Texas State Fish Hatcheries, Management of Prymnesium parvum at Texas State Fish Hatcheries, https://tpwd.texas.gov/publications/pwdpubs/media/pwd_rp_t3200_1138_chapter6.pdf

Southard, G.M., Fries, L.T., Barkoh, A., 2010. Prymnesium parvum the Texas experience. J. Am. Water Res. Assoc. 46, 14-23.

Sunda, W.G., E. Graneli, C.J. Gobler. 2006. Positive Feedback and the Development and Persistence of Ecosystem Disruptive Algal Blooms. J. Phycol. 42: 963–974.

Ulitzur, S., Shilo, M., 1964. A sensitive assay system for determination of the ichthyotoxicity of *Prymnesium parvum*. Journal of General Microbiology. 36:161–169.

United States Environmental Protection Agency, 2002. Methods for Measuring Acute Toxicity of Effluents and Receiving Waters to Freshwater and Marine Organisms. EPA-821-R-02–012. Office of Research and Development, Washington, DC.

Utermöhl, H., 1958. Zur Vervollkommnung der quantitativen Phytoplankton Methodik. Mitt. Int. Ver. Theor. Angew. Limnol. 9, 1-38.

Valenti, Theodore W., Jr. , Susan V. James, Mieke J. Lahousse, Kevin A. Schug, Daniel L. Roelke, James P. Grover, Bryan W. Brooks. 2010. A mechanistic explanation for pH-dependent ambient aquatic toxicity of Prymnesium parvum carter. Toxicon 55 990–998.

VanLandeghem, M.M., M. Farooqi, B. Farquhar, and R. Patiño. 2013. Impacts of Golden Alga *Prymnesium parvum* on fish populations in reservoirs of the upper Colorado River and Brazos River basins, Texas. Transactions of the American Fisheries Society. 142: 581–595.

Villalon, A., Lynch, A., Awwad, H., Gooch, T., Albright, J. 1998. Galveston Bay Freshwater Inflows Study, Technical Memorandum, Trans-Texas Water Program, Southeast Area.

Wetzel, R.G., Likens, G.E., 1991. Limnological Analysis, second ed. Springer-Verlag, New York, pp. 152–155.

CHAPTER V

CONCLUSION

Systems with diverse populations may be more resilient against environmental changes that could alter or negatively impact them (Peterson et al. 1998, Awiti 2011). I show here that diversity of life history traits among species can increase assemblage resistance to the negative effect of an allelopathic species. Sometimes this diversity of life history traits promotes the organization of species into clusters whose competitive similarity is a robust defense against possible invasions by allelopathic species. Indeed, the population dynamics required to maintain high diversity may necessitate the coexistence of specific competitors in an assemblage (Roelke and Eldridge 2008). Certain life history traits in plants have predictive value for allelopathic potential, and allelopathy is likely a common, or at least not uncommon, feature among plants (Meiners 2014). Allelopathy is likely a constant feature of aquatic systems as well, steadily shaping plankton succession dynamics. Over time, aquatic ecologists may amend the view of allelopathy as strictly negative, instead viewing it as a feature whose presence is necessary to sustain biodiversity.

Sustained alterations to our lakes and estuaries, however, may magnify the negative effects of natural competitive interactions such as allelopathy. Whereas dynamic resource environments created by fluctuating environmental conditions such as inflows or high plankton grazing facilitates the coexistence of multiple species by extending a niche gradient, a lack of disturbance or low disturbance decreases diversity and richness (Tilman, 1982; Roelke and Eldridge 2008). Such reduced assemblage diversity increases the opportunity for other species to invade newly opened gaps in a niche gradient (Scheffer and Van Nes, 2006; Vallina et al., 2014).

In aquatic systems, a reduction in phytoplankton diversity can lessen the stabilizing effects of interspecific competition, resulting in more frequent harmful blooms.

References

Awiti, A. 1998. Biological Diversity and Resilience: Lessons from the Recovery of Cichlid Species in Lake Victoria. Ecology and Society, Vol 16:1

Peterson, Garry D.; Allen, Craig R.; and Holling, C. S., "Ecological Resilience, Biodiversity, and Scale" (1998). Nebraska Cooperative Fish & Wildlife Research Unit -- Staff Publications. http://digitalcommons.unl.edu/ncfwrustaff/4 Meiners, S. 2014. Functional correlates of allelopathic potential in a successional plant community. Plant Ecol (2014) 215:661–672.

Roelke, D.L., Eldridge, P.M., 2008. Mixing of supersaturated assemblages and the precipitous loss of species. Am. Nat. 171, 162–175.

Scheffer, M. and E.H. van Nes. 2006. Self-organized similarity, the evolutionary emergence of groups of similar species. Proceedings of the National Academy of Sciences. 103(16): 620-6235.

Sunda, W., Edna Graneli and Christopher J. Gobler. 2006. Positive Feedback and the Development and Persistence of Ecosystem Disruptive Algal Blooms. Journal of Phycology, 42:5, 963-974.

Tilman, David. Resource competition and community structure. 1982. Princeton University Press.

Vallina, S. M., Word, B. A., Dutkiewicz, S. & Follows, M. J. 2014. Maximal feeding with active prey-switching: A kill-the-winner functional response and its effect on global diversity and biogeography. Prog. Oceanogr. 120, 93–109.

APPENDIX A

Tri-panel graphs for the seven lake systems which includes biovolume density over time for total phytoplankton and the sum of all allelopathic taxa (top), the number of taxa occurring in each of the standardized size classes over time (middle), and the average number of species clusters observed over time (bottom).

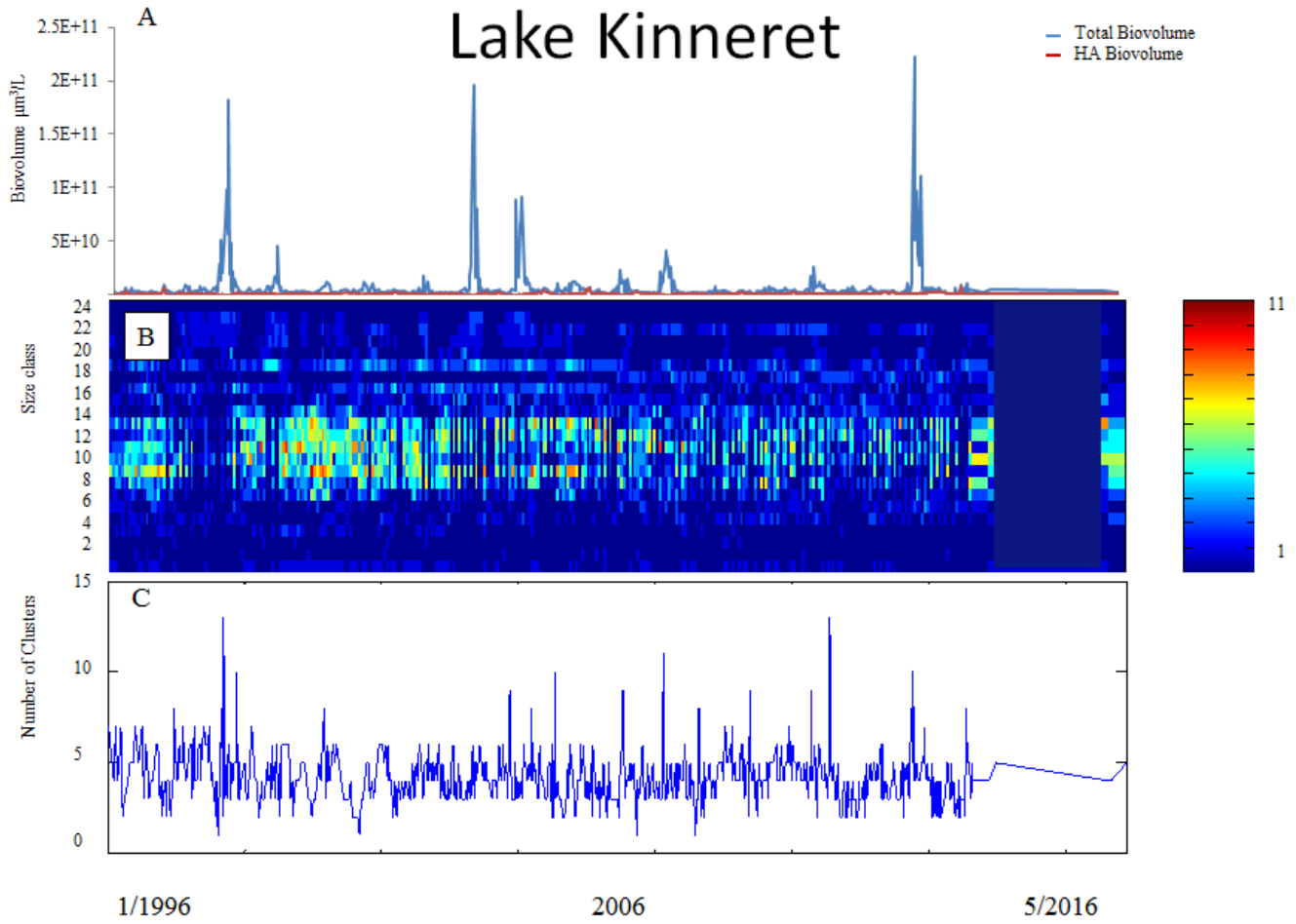

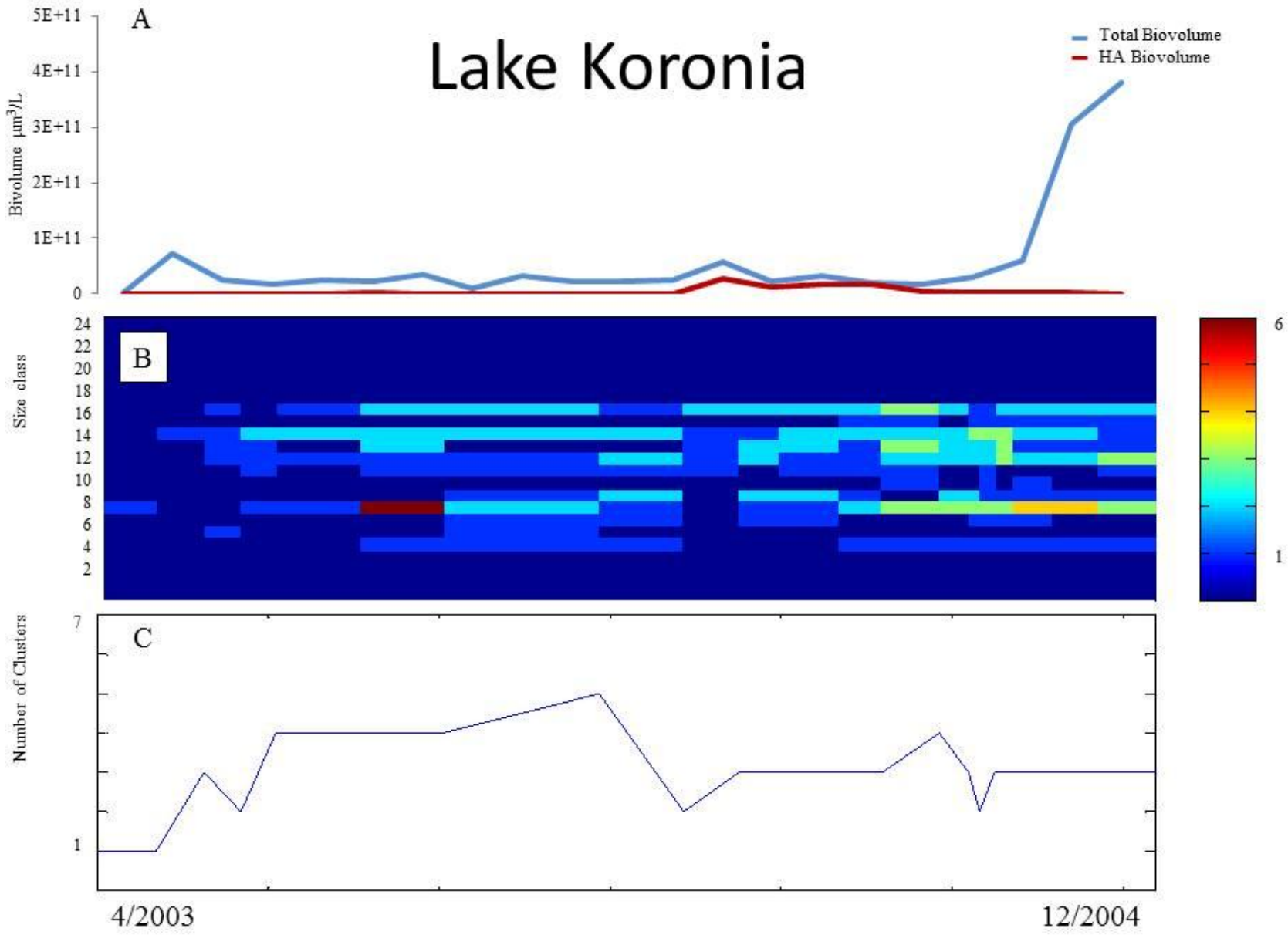
A
Lake Koronia
Total Biovolume
HA Biovolume
Bivolume µm³/L
5E+11
4E+11
3E+11
2E+11
1E+11
0
B
Size class
24
22
20
18
16
14
12
10
8
6
4
2
6
1
C
Number of Clusters
7
1
4/2003
12/2004

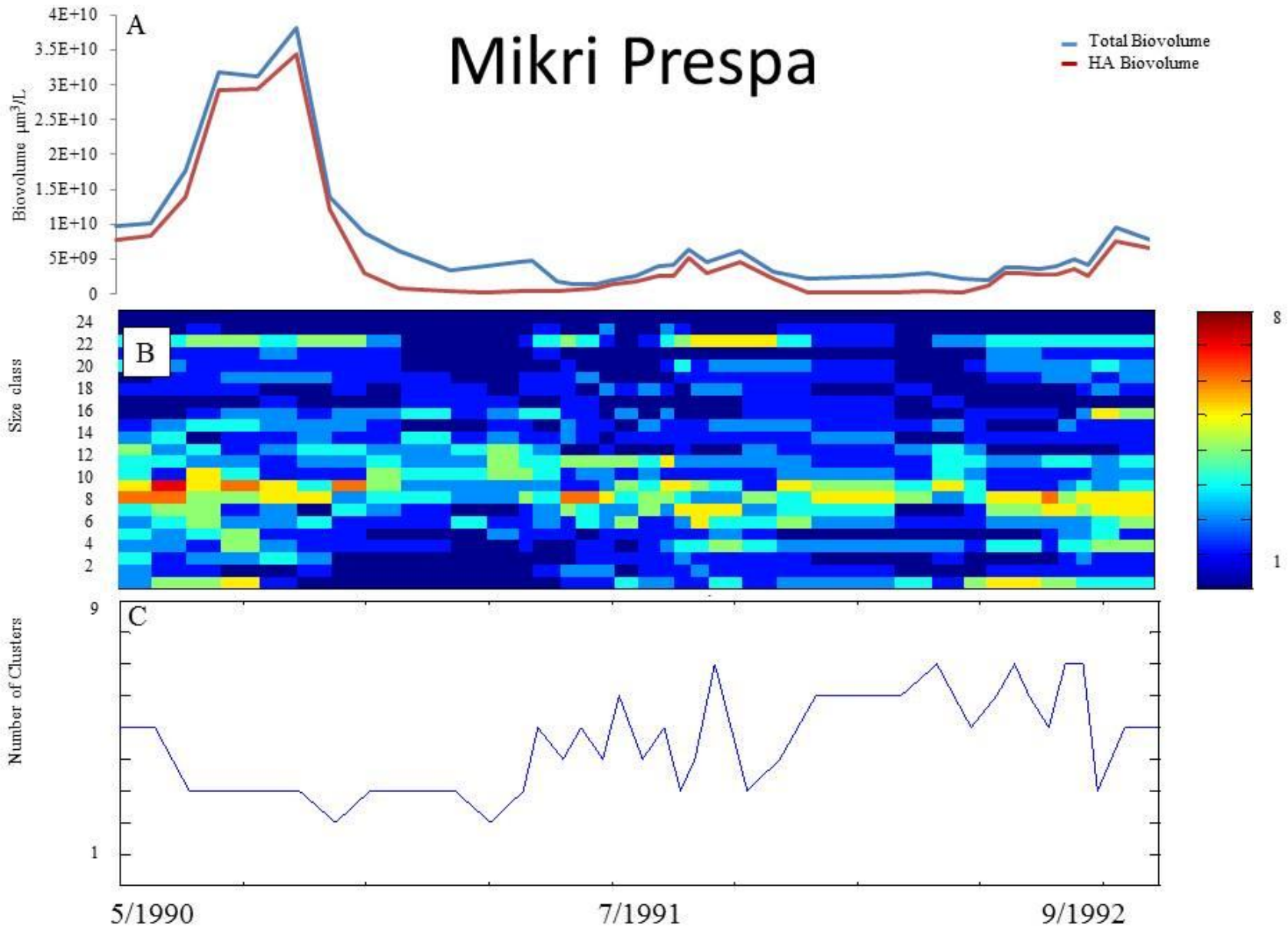
Mikri Prespa
A
Total Biovolume
HA Biovolume
Biovolume µm³/L
4E+10
3.5E+10
3E+10
2.5E+10
2E+10
1.5E+10
1E+10
5E+09
0
B
Size class
24
22
20
18
16
14
12
10
8
6
4
2
8
1
C
Number of Clusters
9
1
5/1990
7/1991
9/1992

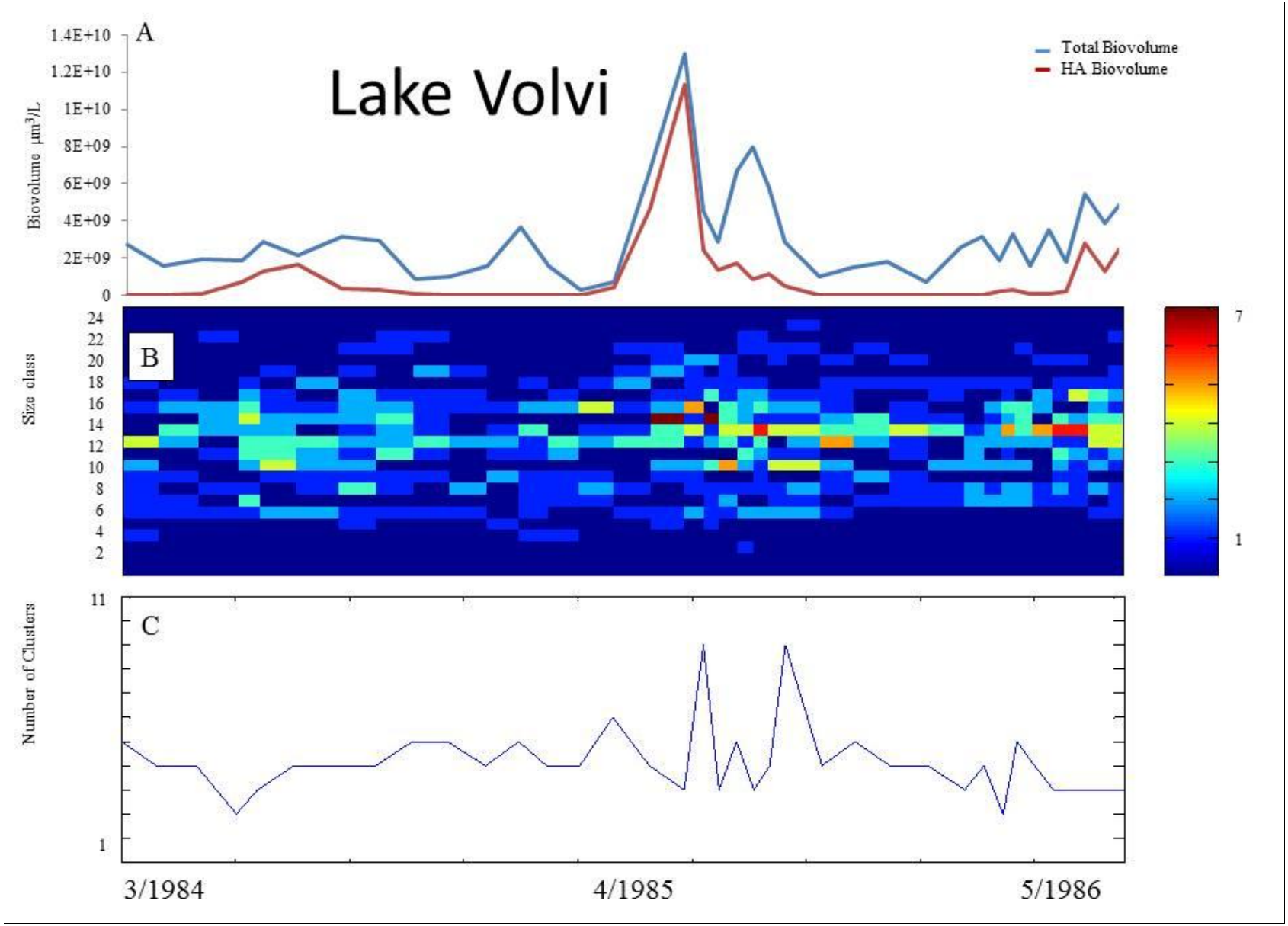
A
Lake Volvi
Total Biovolume
HA Biovolume
Biovolume µm³/L
1.4E+10
1.2E+10
1E+10
8E+09
6E+09
4E+09
2E+09
0
B
Size class
24
22
20
18
16
14
12
10
8
6
4
2
7
1
C
Number of Clusters
11
1
3/1984
4/1985
5/1986

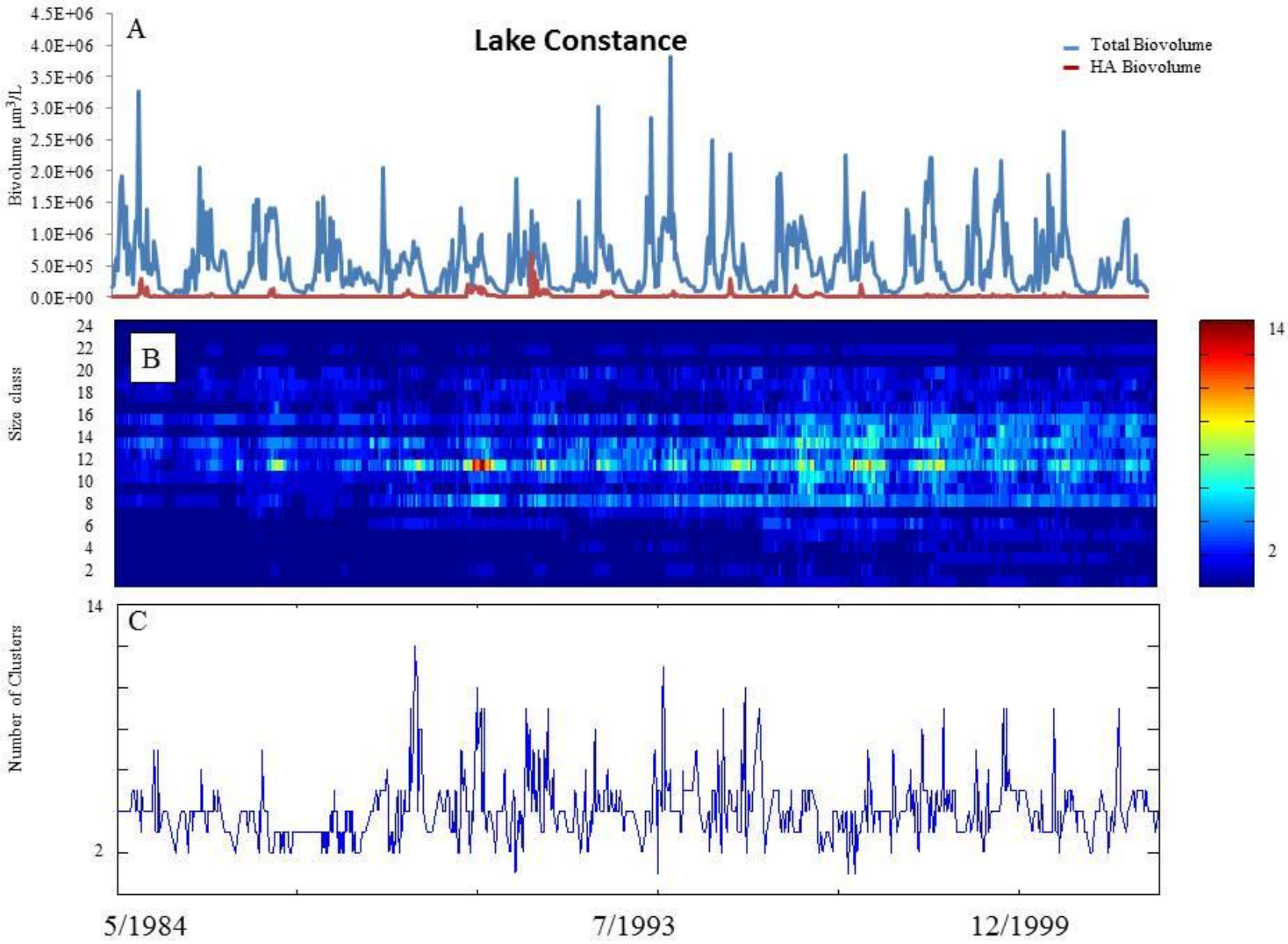
A
Lake Constance
Total Biovolume
HA Biovolume
Bivolume µm³/L
4.5E+06
4.0E+06
3.5E+06
3.0E+06
2.5E+06
2.0E+06
1.5E+06
1.0E+06
5.0E+05
0.0E+00
B
Size class
24
22
20
18
16
14
12
10
8
6
4
2
14
2
C
Number of Clusters
14
2
5/1984
7/1993
12/1999

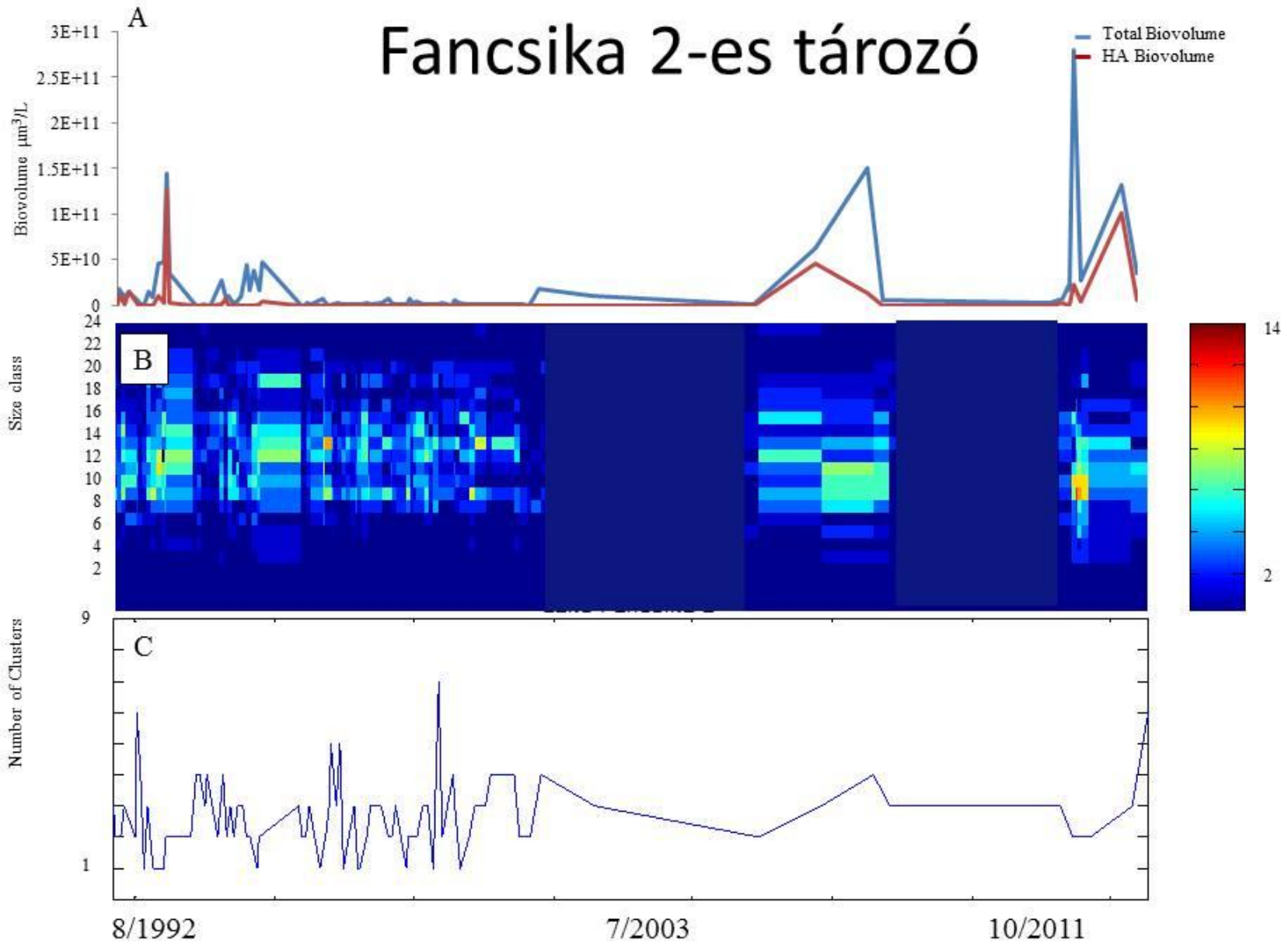
Fancsika 2-es tározó
A
Total Biovolume
HA Biovolume
Biovolume µm³/L
3E+11
2.5E+11
2E+11
1.5E+11
1E+11
5E+10
0
B
Size class
24
22
20
18
16
14
12
10
8
6
4
2
14
2
C
Number of Clusters
9
1
8/1992
7/2003
10/2011

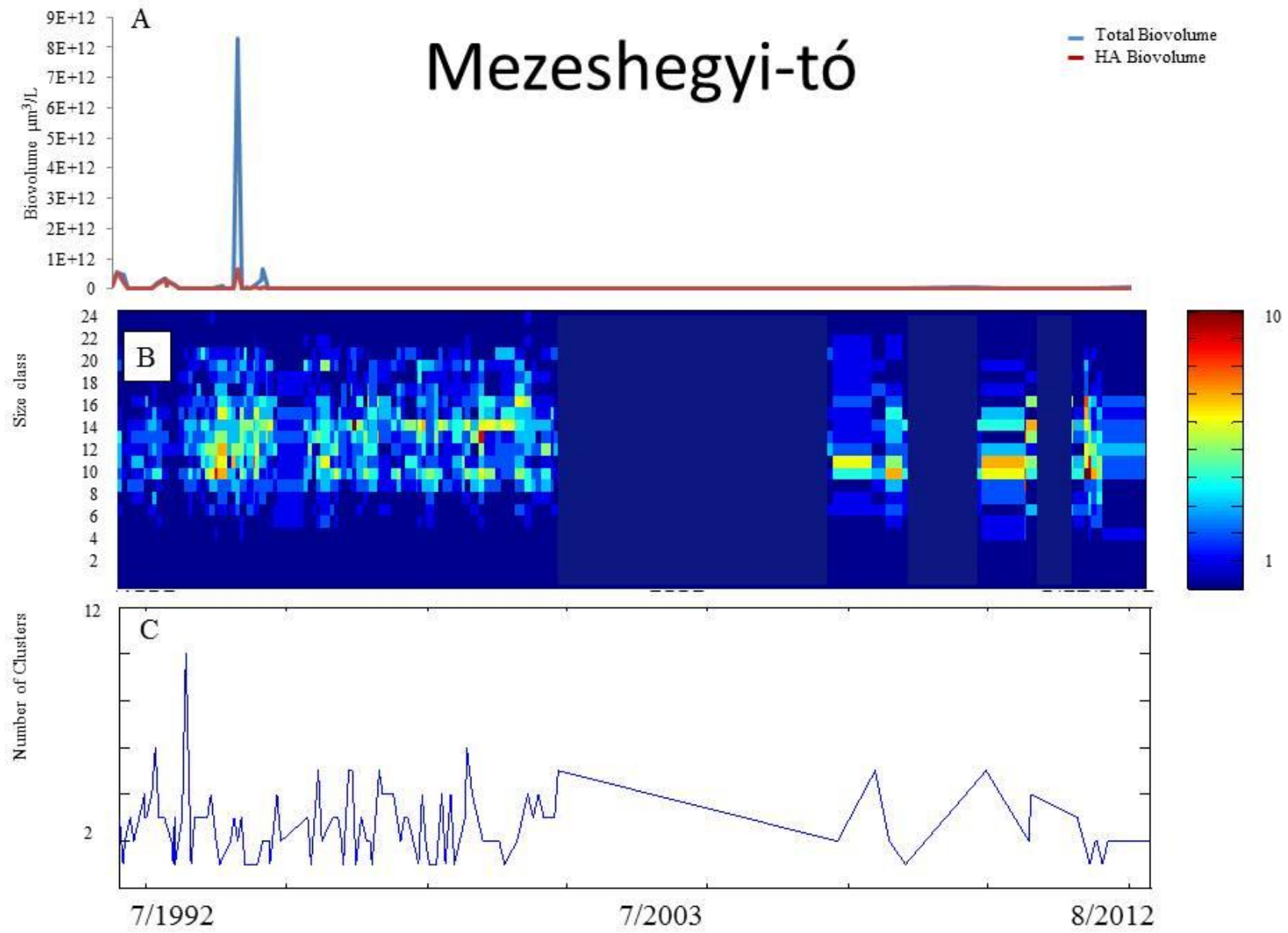
Mezeshegyi-tó
A
Total Biovolume
HA Biovolume
Biovolume µm³/L
9E+12
8E+12
7E+12
6E+12
5E+12
4E+12
3E+12
2E+12
1E+12
0
B
Size class
24
22
20
18
16
14
12
10
8
6
4
2
10
1
C
Number of Clusters
12
2
7/1992
7/2003
8/2012

APPENDIX B

Measured levels of pH at each time point before manipulation for that time point. Yellow dotted line is target pH. Top panels are filtered treatments, bottom panels are unfiltered treatments. Black, turquoise and red lines are stationary treatments; gray, blue and orange lines are log treatments. The graphs in order from the left are Galveston Bay fall, Matagorda Bay fall, Galveston Bay winter, Matagorda Bay winter.